

NASA TECHNICAL NOTE



NASA TN D-7777

NASA TN D-7777

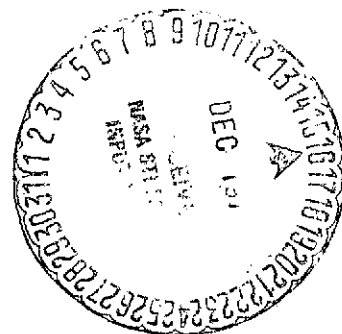
(NASA-TN-D-7777) A MOTION-CONSTRAINT  
LOGIC FOR MOVING-BASE SIMULATORS BASED ON  
VARIABLE FILTER PARAMETERS (NASA) 55 P  
HC \$4.25 CSCL 01B

N75-11933

Unclas  
H1/05 03964

# A MOTION-CONSTRAINT LOGIC FOR MOVING-BASE SIMULATORS BASED ON VARIABLE FILTER PARAMETERS

*G. Kimball Miller, Jr.*  
*Langley Research Center*  
*Hampton, Va. 23665*



1. Report No. NASA TN D-7777		2. Government Accession No.		3. Recipient's Catalog No.	
4. Title and Subtitle A MOTION-CONSTRAINT LOGIC FOR MOVING-BASE SIMULATORS BASED ON VARIABLE FILTER PARAMETERS				5. Report Date December 1974	
				6. Performing Organization Code	
7. Author(s) G. Kimball Miller, Jr.				8. Performing Organization Report No. L-9585	
9. Performing Organization Name and Address NASA Langley Research Center Hampton, Va. 23665				10. Work Unit No. 504-29-14-01	
				11. Contract or Grant No.	
12. Sponsoring Agency Name and Address National Aeronautics and Space Administration Washington, D.C. 20546				13. Type of Report and Period Covered Technical Note	
				14. Sponsoring Agency Code	
15. Supplementary Notes					
16. Abstract <p>A motion-constraint logic for moving-base simulators has been developed that is a modification to the linear second-order filters generally employed in conventional constraints. In the modified constraint logic, the filter parameters are not constant but vary with the instantaneous motion-base position to increase the constraint as the system approaches the positional limits. With the modified constraint logic, accelerations larger than originally expected are limited while conventional linear filters would result in automatic shutdown of the motion base. In addition, the modified washout logic has frequency-response characteristics that are an improvement over conventional linear filters with braking for low-frequency pilot inputs. During simulated landing approaches of an externally blown flap short take-off and landing (STOL) transport using decoupled longitudinal controls, the pilots were unable to detect much difference between the modified constraint logic and the logic based on linear filters with braking.</p>					
17. Key Words (Suggested by Author(s)) Motion compensation Washout Moving-base simulation				18. Distribution Statement Unclassified -- Unlimited  STAR Category 05	
19. Security Classif. (of this report) Unclassified	20. Security Classif. (of this page) Unclassified	21. No. of Pages 53	22. Price* \$4.25		

# A MOTION-CONSTRAINT LOGIC FOR MOVING-BASE SIMULATORS BASED ON VARIABLE FILTER PARAMETERS

By G. Kimball Miller, Jr.  
Langley Research Center

## SUMMARY

A motion-constraint logic for moving-base simulators has been developed that is a modification to the linear second-order filters generally employed in conventional constraints. In the modified constraint logic, the filter parameters are not constant but vary with the instantaneous motion-base position to increase the constraint as the system approaches the positional limits. With the modified constraint logic, accelerations larger than originally expected are limited while conventional linear filters would result in automatic shutdown of the motion base. In addition, the modified washout logic has frequency-response characteristics that are an improvement over conventional linear filters with braking for low-frequency pilot inputs. During simulated landing approaches of an externally blown flap short take-off and landing (STOL) transport using decoupled longitudinal controls, the pilots were unable to detect much difference between the modified constraint logic and the logic based on linear filters with braking.

## INTRODUCTION

The desirability of simulator motion on flight-training devices is widely accepted. In advanced aircraft research fixed-base simulators have been quite useful, although trained pilots are generally required to extrapolate the aircraft behavior from that of the simulator. The degree of extrapolation required can be reduced through the judicious use of motion cues. The kind and amount of motion required, however, is not well defined. In most cases the available travel of the motion base is small compared to that of the simulated aircraft maneuver. Consequently, it is necessary to design a motion constraint or washout logic to avoid reaching the physical limits of the motion system.

Early motion-constraint work generally concerned simulators with limited degrees of freedom (refs. 1, 2, and 3) and either scaled the aircraft accelerations or used second-order linear filters to restrict the base motion. As motion systems with multiple degrees of freedom became more prevalent, the practice generally has been to employ second-order linear filters to the accelerations associated with each degree of freedom while coordinating the angular and translational degrees of freedom to obtain improved

acceleration representation. For example, the onset of a given longitudinal aircraft acceleration is obtained from motion along the longitudinal axis of the motion base, while the sustained part of the aircraft acceleration is obtained by tilting the base in pitch to use a gravitational component. This "coordinated" approach is typified by reference 4 and will be referred to herein simply as washout. This type of motion constraint does not guarantee that the simulator-position commands will be bounded, however. Consequently, Schmidt and Conrad added a braking acceleration procedure to the conventional constraint logic of reference 4. The procedure basically consists of limiting acceleration commands above the motion-base capabilities to the acceleration limits, and simultaneously maintaining the position and velocity limits by means of a position-velocity boundary that is based on the acceleration and position limits and the computed current position of the base. The result is reported in reference 5 and will be referred to herein as washout-with-braking. Washout-with-braking has been adapted to the Langley visual-motion simulator (VMS) in reference 6. The position limits of the VMS vary considerably with base displacement from the null position due to the synergistic nature of the system. Reference 6 consequently included a method to predict the translation position limits based on the current orientation of the base. The method essentially predicts the limits of the translational degrees of freedom through the inverse actuator transformation reported in reference 7. A precise motion envelope for the VMS can, of course, never be described because of the infinite number of combinations of displacements in the six degrees of freedom.

The present paper concerns a modification to the washout logic wherein the linear filter parameters are not constant but are functions of the current distance from the position limit for the particular degree of freedom. In addition, the modified washout logic employs a simple prediction of the lateral and longitudinal position limits based on the vertical position of the motion base. The washout and modified-washout logics are briefly compared through their performance in limiting the motion-base response to the airplane motions recorded on tape during the flight of an experimental short take-off and landing (STOL) transport aircraft. The modified-washout logic is then compared with the washout-with-braking logic, with a pilot in the control loop, using the VMS to simulate the landing and approach of an externally blown jet flap STOL transport aircraft.

## SYMBOLS

Measurements and calculations were made in U.S. Customary Units. They are presented herein in the International System of Units (SI) with the equivalent values given parenthetically in the U.S. Customary Units.

$\bar{a}$	acceleration vector measured at center of gravity of airplane, meters/sec <sup>2</sup> (ft/sec <sup>2</sup> )
$a_x, a_y, a_z$	acceleration components in body axes at location of pilot's seat, meters/sec <sup>2</sup> (ft/sec <sup>2</sup> )
$a'_x, a'_y, a'_z$	acceleration components at simulated pilot's seat without coordinated tilting for sustained accelerations, meters/sec <sup>2</sup> (ft/sec <sup>2</sup> )
$g$	acceleration at surface of Earth due to gravitational attraction, 9.81 meters/sec <sup>2</sup> (32.2 ft/sec <sup>2</sup> )
$h$	altitude, meters (ft)
$K_k$	scaling parameter
$P_k$	phase angle relating output acceleration to input acceleration, radians or degrees
$p, q, r$	angular velocities about airplane longitudinal, lateral, and vertical axes, respectively, radians/sec
$s$	Laplace operator
$u, v, w$	airplane translational velocities along airplane longitudinal, lateral, and vertical axes, respectively, meters/sec (ft/sec)
$\dot{u}_m, \dot{v}_m, \dot{w}_m$	components of $\bar{a}$ measured along airplane longitudinal, lateral, and ver- tical axes, respectively
$V$	airspeed, meters/sec (ft/sec)
$x, y, z$	displacements from reference position in inertial coordinates, meters (ft)
$x_p$	displacement of pilot's seat along airplane longitudinal axis from airplane center of gravity, meters (ft)
$y$	airplane displacement from running center line, meters (ft)

$\alpha$	airplane angle of attack, degrees
$\beta$	airplane angle of sideslip, degrees
$\Gamma_{a,i}$	transformation matrix from airplane body axes to inertial axes
$\gamma$	airplane flight-path angle, degrees
$\delta_a$	aileron deflection, positive for right roll, degrees
$\delta_r$	rudder deflection, degrees
$\delta_s$	asymmetric deflection of spoilers, positive for right roll, degrees
$\delta_t$	horizontal tail deflection, degrees
$\xi_k$	damping ratio
$\theta', \varphi'$	components of motion-base pitch and roll angles due to tilting base to provide sustained linear acceleration, radians or degrees
$\tau_k$	time constant of first-order filter, sec
$\psi, \theta, \varphi$	Euler angles of rotation relating airplane body axes and inertial axes, radians or degrees
$\psi_{bo}, \theta_{bo}, \varphi_{bo}$	components of motion-base angles of yaw, pitch, and roll, respectively, due to high-frequency content of airplane angular accelerations, radians or degrees
$\omega_k$	forcing frequency, radians/sec
$\omega_{nk}$	break frequency of washout filter, radians/sec

**Subscripts:**

b            refers to motion base

c	refers to pilot inputs to decoupled control system
k	denotes corresponding washout filter where $k = x, y, z, r, p, \gamma, \psi, \theta, \text{ or } \varphi$
max	maximum
0	denotes linear filter values

Abbreviation:

STOL      short take-off and landing

A dot over a variable denotes the time derivative of that variable, and two dots indicate second derivative.

## MOTION-BASE RESTRICTIONS

A basic problem in developing motion-constraint logic for the Langley visual-motion simulator (VMS) (fig. 1) concerns the definition of the performance limits of the motion base. The motion base cannot exceed design physical limits on position, velocity, or acceleration for each of the six degrees of freedom. The normal performance limits of the motion base in each degree of freedom (operating independently) from a neutral position 2.58 m (8.46 ft) above the floor, as given by the manufacturer's specifications, are given in table I. The synergistic design of the motion base, however, causes the position limits to be so interrelated so that displacements about any axis become more limited as the displacement about some other axis increases. For example, the motion in the  $x_b$ - $y_b$  plane becomes more restrictive as the  $z_b$  position changes from the null position (fig. 2). Because the  $x_b$ - $y_b$  envelope is of a fairly complex shape, a motion envelope consisting of an inscribed square was assumed (fig. 2) for the modified constraint logic of the present study. The resulting permissible travel is shown in figure 3 as a function of vertical position  $z_b$ .

## WASHOUT LOGIC

The washout logic employs linear filtering of the airplane accelerations in order to avoid sustained motion-base velocities. The second-order high-pass linear filters are of the form exemplified by the longitudinal channel

$$\frac{\ddot{x}_b}{\ddot{x}} = \frac{K_X s^2}{s^2 + 2\zeta_X \omega_{n_X} s + \omega_{n_X}^2} \quad (1)$$

where  $s$  denotes the Laplace operator. The dynamic response of this type of filter is presented in figure 4 for  $K_x$  of 1.0. A simplified method (ref. 8) for estimating the initial values for the iterative process of finding the break frequencies  $\omega_{n_x}$  for a given task is based upon the steady-state solution of the linear second-order system. Substituting  $s^2 x_b$  for  $\ddot{x}_b$  in equation (1) and canceling the  $s^2$  term in the numerators yields the steady-state solution

$$\frac{x_b}{\ddot{x}} = \frac{K_x}{s^2 + 2\zeta_x \omega_{n_x} s + \omega_{n_x}^2} \bigg|_{s=0} = \frac{K_x}{\omega_{n_x}^2} \quad (2)$$

from which  $\omega_{n_x}$  can be determined as a function of scaling  $K_x$  and expected airplane acceleration  $\ddot{x}$  for the existing base limit  $x_b$ . The choice of damping coefficient  $\zeta_x$  involves a compromise between the desire for small phase angles, which requires small values of  $\zeta_x$  (fig. 4), and the desire for unamplified motion, which requires  $\zeta_x$  greater than about 0.7. The relationship between phase angle  $P_x$  and the damping parameter  $\zeta_x$ , which can be obtained from equation (1) for a sinusoidal input frequency  $\omega_x$  by setting  $s$  equal to  $i\omega_x$ , is

$$\zeta_x = \frac{1}{2} \left( \frac{\omega_x}{\omega_{n_x}} - \frac{\omega_{n_x}}{\omega_x} \right) \tan P_x \quad (3)$$

Piloted simulator experience indicates that the phase angle should be less than about  $20^\circ$  for sinusoidal input frequencies up to 10 radians per second (ref. 9). It is, however, impossible to maintain small phase angles for inputs with low frequencies (fig. 4).

#### Coordination of Translational and Rotational Motion

As multiple degree-of-freedom motion bases have come into being, the use of motion-base tilt to represent sustained linear accelerations using a component of gravity has become prevalent (see refs. 4 and 9). This technique is referred to as coordinated washout. Coordination is an integral part of the washout logic which is used in the present study and depicted in figure 5.

The acceleration components that would be felt by a pilot located at the aircraft center of gravity are  $\dot{u}_m$ ,  $\dot{v}_m$ , and  $\dot{w}_m$  along the aircraft longitudinal, lateral, and vertical axes, respectively. When the pilot is located ahead of the center of gravity, additional accelerational components  $-(q^2 + r^2)x_p$ ,  $(\dot{r} + pq)x_p$ , and  $(pr - \dot{q})x_p$  must be added to  $\dot{u}_m$ ,  $\dot{v}_m$ , and  $\dot{w}_m$  (fig. 5). Sustained translational accelerations are represented by tilting the pilot and using the gravity vector to produce the cue. For example, a sustained longitudinal acceleration is simulated by tilting the motion base in



pitch. The acceleration then felt by the subject is

$$a_x = -g \sin \theta_b$$

or, for small angles,

$$\frac{a_x}{g} = -\theta'$$

This tilting is accomplished by dividing the accelerations  $a_x$  and  $a_y$  by  $g$  and passing the result through low-pass filters to obtain the tilt angles  $\theta'$  and  $\varphi'$ , respectively (fig. 5). The rotation rates to attain these tilt angles must, however, be made at levels below the pilot's angular-motion threshold in order to avoid erroneous cues. Consequently, relatively small savings are actually attainable when the sustained accelerations  $g\theta'$  and  $g\varphi'$  are subtracted from the aircraft translational accelerations. Similarly, an attempt to represent a desired rotational cue by means of base rotation alone would result in a false translational cue because of temporary misalignment of the gravity vector. Consequently, a translational correction is used (fig. 5) to offset the erroneous cue induced by rotational motion. The resulting translational accelerations are transferred to an inertial system of axes and passed through the high-pass filters to limit motion-base travel in order to avoid the motion-system limits. Although angular motions often are constrained through the use of first-order, high-pass filters, the current study uses second-order filters.

#### Application of Washout Logic

In order to examine the washout logic under realistic conditions, motion calculations were made using, as inputs, some flight data from an XC-142 aircraft performing a wind-up turn (coordinated turn with increasing vertical acceleration). The scaling parameters  $K_k$ ,  $K_p$ , and  $K_r$  were chosen to be unity. The remaining parameters,  $\omega_{nk}$  and  $\zeta_k$ , were established using equations (2) and (3), the motion-base limits (table I), the requirement that phase angles be less than  $20^\circ$  when possible, and the maximum expected translational and rotational accelerations. The aircraft maximum acceleration levels, after removal of the  $1g$  vertical acceleration bias due to gravity, were

$$\ddot{x} = \ddot{y} = 0.5 \text{ m/sec}^2 \text{ (1.62 ft/sec}^2\text{)}$$

$$\ddot{z} = 5.89 \text{ m/sec}^2 \text{ (19.32 ft/sec}^2\text{)}$$

$$\ddot{\psi} = \ddot{\theta} = 30^\circ/\text{sec}^2$$

The computed response of the motion base to the XC-142 wind-up turn flight tape is presented in figure 6 referenced to a straight and level trim condition. With no washout (or constraint logic), not only the translational positions but also the translational velocities relative to the trim conditions quickly violate the motion-base limits. This violation is particularly critical for the vertical channel where the initial acceleration level causes the position and velocity limits to be violated in less than 1 second. When the washout logic is applied, the translational velocities and positions are well within the performance limits of the motion base. This limiting is accomplished by rapidly washing out the sustained accelerations while accurately reproducing the high-frequency variations.

The angular positions and velocities quickly violate the motion-base limits when no washout is used, primarily because of biases in the angular accelerometer readings. The washout logic effectively eliminates these biases so that the motion-base limits are not violated. A second example of the effectiveness of the washout in eliminating biases is presented in figure 7 for the case when a pitch doublet was performed by the aircraft.

#### MODIFIED WASHOUT LOGIC

The motion cues resulting from the washout logic could be maximized if it were known that the accelerations would never exceed a given level. Such is not the case. Pilots occasionally make control inputs which result in acceleration spikes that are considerably larger than those expected for the normal performance of a given task. The large accelerations result in the motion base hitting its limits, a condition which the pilots do not like. Because the maximum accelerations are not accurately predictable, the motion constraints are usually tightened to avoid hitting the limits at even the largest acceleration spikes. Tightening the motion constraints results in the inefficient use of the motion system over the majority of the flight. Consequently, new techniques are being used that involve braking procedures, which are the subject of the present paper. In this study a modified washout logic was developed that uses break frequencies and damping ratios that are not constants but are functions of the instantaneous or current base position. The base-line or zero displacement values for the modified constraint logic are the same as the constant values previously determined for the washout logic. Because the  $x_b$ - $y_b$  envelope is not constant but varies (fig. 2) with the vertical  $z_b$  position of the base, however, the base-line values of the damping ratios and break frequencies of the  $x_b$  and  $y_b$  channels are given as functions of  $z_b$  (see fig. 8). In order to provide the desired additional constraint, the break frequencies have been determined as functions of the current base positions (figs. 9 and 10) with damping ratios chosen in an attempt to meet the  $20^\circ$  phase requirement for sinusoidal input frequencies up to 10 radians per second, as previously noted. The filter parameters for the three angular

channels and the vertical channel are presented in figure 9 (based on XC-142 flight-tape input values) as functions of the absolute value of the current base position. The angular position limits were not varied as functions of  $z_b$  because only small angular displacements were expected for STOL type transport maneuvers. The variation of the filter parameters in the longitudinal and lateral directions is presented in figure 10 as a function of the absolute value of the current base positions and the maximum permissible travel. Consequently, as the base moves toward its limits, the break frequencies increase to provide stronger constraints. As the break frequencies increase, the damping ratios required to minimize the phase angle approach zero. The damping ratios (figs. 9 and 10), however, have been limited to nonzero minimum values to keep the motion base from undamped oscillations when at large displacements from the null position.

### APPLICATION OF MODIFIED WASHOUT LOGIC

For the XC-142 wind-up turn flight data, the computed motion-base accelerations, velocities, and displacements resulting from the modified constraint logic were imperceptibly different from those presented in figure 6 for the washout logic. This small difference occurs because the base values of the variable filter parameters of the modified constraint logic were equal to the constant filter parameters of the washout logic, and because the flight data contained no sustained accelerations that would cause the motion base to operate near its position limits. The advantages of the modified constraint logic become apparent when greater demands are placed upon the system. An example of the input accelerations being greater than expected has been generated from the wind-up turn tape by considering the case where the pilot is not at the aircraft center of gravity, as has been assumed thus far, but is 30.48 meters (100 ft) forward of the center of gravity (see fig. 11). This case also illustrates the shift in importance from angular cues to translational cues as the separation distance  $x_p$  from the center of gravity to the pilot's station increases. Increasing  $x_p$  causes the lateral and vertical accelerations to increase (compare figs. 6 and 11) proportionally with yaw and pitch acceleration, respectively. When the washout logic is employed (fig. 11), the lateral acceleration has increased to the extent that the lateral position limit of the motion system is violated after approximately 6 seconds. In an operational case, the motion base would be shut down at this point. When the modified washout logic is used (fig. 12), however, the lateral travel of the motion system remains well within the system limits. The modified washout logic was incorporated in a moving-base simulation study so that a subjective pilot evaluation could be obtained.

## SIMULATOR APPLICATION

The Langley visual-motion simulator (VMS) achieves motion in each degree of freedom through a combination of actuator extensions rather than independent drive systems for each degree of freedom. This synergistic aspect of the VMS necessitated the actuator extension and inverse transformation software described in reference 7. The constraint logic chosen for the basic VMS simulation work is a second generation version (added braking acceleration procedure) of Schmidt and Conrad's coordinated washout technique (ref. 5), specifically adapted for the VMS (ref. 6). This washout technique is referred to as the washout-with-braking logic. It has been applied to the study of simulated STOL aircraft landing approaches (previously reported in ref. 10 for a fixed-base study) in order to obtain a basis for evaluating the modified washout with a pilot in the control loop. The pilot's task was to assume control of an externally blown flap STOL transport approximately 1 minute prior to landing and to use decoupled longitudinal and lateral control systems to touch down in a 137.2-meter-long (450-ft) area with sink rates that were as small as possible. The decoupled longitudinal control system (ref. 10) used the column to command flight-path angle, the flap lever to command pitch angle, and the throttle lever to control forward velocity. The decoupled lateral controls used the wheel to command yaw rate and the rudder pedals to command sideslip angle. The washout parameters used in the washout-with-braking logic for the decoupled STOL transport simulation are presented in table II.

The basic STOL task, a straight-in approach and landing, involves operation of the aircraft at essentially constant attitude when decoupled longitudinal controls are used (see ref. 10). Consequently, the modified washout logic was applied only to the translational degrees of freedom of the STOL simulation. The application included removing the braking acceleration circuit of reference 6 and using the variable washout parameters (figs. 9(a) and 10) to constrain the translational degrees of freedom. The limit prediction technique of reference 6 was also removed, being replaced by the fixed boundary approximations shown in figure 2.

### Constraint Logic Comparison

An example of the control response of the externally blown flap STOL transport with a decoupled longitudinal control system is presented in figure 13. A  $2^\circ$  per second change in  $\gamma_c$  is initiated approximately 6 seconds into the flight and is maintained for about 2 seconds. Approximately 16 seconds into the flight a step input of 12 m/sec (40 ft/sec) in forward velocity is commanded. After 32 seconds into the flight a rapid  $4^\circ$  change in pitch attitude is commanded. Because the aircraft is quite sluggish, 6 seconds were required to reach the commanded pitch angle at which time a pitch angle of

about  $-1^\circ$  was commanded. The decoupled longitudinal control system provided smooth, well-damped control over the aircraft and was well received by the research pilots in the fixed-base simulation study (ref. 10).

The computed response of the motion base to the acceleration profile of figure 13 is presented in figure 14 for both the washout-with-braking and the modified washout logic. There is little difference between the acceleration profiles using the washout-with-braking logic with its position prediction technique and the modified washout logic with its simple representation of the  $x$  and  $y$  limits of the base. The longitudinal and vertical displacements, however, are noticeably smaller in the case of the modified washout logic. The pilots were unable to detect any difference between the two constraint logics, but found the motion in either case to be unacceptable because of erroneous accelerations produced whenever the legs of the motion base reversed their direction of motion. These turn-around bumps could be effectively masked by adding low-level turbulence to the flight simulation. The turbulence model used in this study was based on the Dryden spectral form having a root-mean-square (rms) value of 0.3 m/sec (1 ft/sec). The time history of a typical landing approach made in low-level turbulence is presented in figure 15. The pilot assumes command of the simulated STOL aircraft in level flight at an altitude of 243.8 meters (800 ft). Approximately 8 seconds into the flight the pilot commanded a  $-6^\circ$  flight-path angle which he maintained until about 55 seconds into the flight, at which time a transition to  $-4^\circ$  flight-path angle was commanded. At 75 seconds the pilot initiated a flare maneuver and touched down with a sink rate of about 1.2 m/sec (4 ft/sec). With the use of low-level turbulence, the pilots believed the motion to be adequate and again could not distinguish between the washout-with-braking logic and the modified washout logic. The computed motion-base activity for either constraint logic is illustrated in figure 16.

#### Supplemental Investigation

Because the small differences between the washout-with-braking logic and the modified washout logic were not detectable by the pilot, a supplementary investigation was performed to examine differences in motion with the two constraint logics. The supplementary investigation used sinusoidal commanded inputs in the column,  $\gamma_c$ , and wheel  $\dot{\psi}_c$ .

The frequency of the sinusoidal forcing functions was varied from 0.5 to 10 rad/sec at amplitudes that ranged from  $1^\circ$  to  $10^\circ$  for flight-path angle and 2 to 20 deg/sec for yaw rate. (The amplitude and frequency remained constant for any given run.) Very little difference existed in acceleration profiles obtained with the two washout techniques. The more noticeable differences between the two washout techniques occurred at low forcing frequencies typified by the time histories presented in figure 17. The small

differences in acceleration profiles shown in figure 17 are too small for the pilots to detect during the piloted landing-approach task.

The filter parameters of the washout techniques were subsequently changed in an attempt to increase the response of the motion base by halving the damping ratio of each channel, while the natural frequencies of the longitudinal and lateral channels were multiplied by 0.7 and that of the vertical channel was multiplied by 0.5. Some results of this phase of the study are illustrated in figure 18 in the form of frequency-response characteristics of the washout techniques applied to the vertical channel. The vertical channel was used in the illustration rather than the longitudinal channel because the longitudinal and pitch channels are coordinated and would unduly complicate the analysis. The amplitude ratio of the response was approximately the same for the two washout techniques when each had its original value of natural frequency and damping, and the ratios were not affected by the magnitude of the control input.

Reducing the base-line values of the filter parameters of the modified washout to  $\omega_{n_z,0} = 1.5$  and  $\zeta_{z,0} = 0.25$  resulted in increased response, particularly at low frequencies, without appreciably changing the phasing (fig. 18). It was of interest to compare the performance of the modified washout with that obtained from linear filters having the same natural frequency and damping. This comparison (fig. 18) shows that the modified washout generally allows more performance than the linear filter, particularly at low frequencies. The advantage of the modified washout over the linear filter is obviously introduced by the reduction of the damping parameter with  $z_b$ -displacement (fig. 8), since the variation of  $\omega_{n_z}$  would by itself tend to restrain the motion.

It should be noted that washout-with-braking is more restrictive than the use of linear filters (having the same filter constants  $\omega_{n_z}$  and  $\zeta_z$ ). Based on the curves of figure 18, therefore, the modified washout technique provides for greater performance than does the washout-with-braking technique, when both techniques use the same base-line values for natural frequency and damping.

It should be emphasized that care must be taken in choosing the base-line values of the modified washout. For example, if the vertical channel were not scaled down (by 0.2), the peak amplitude ratio (fig. 18) would be greater than unity and a magnification of the output would occur. In such a case, the original base-line filter parameters (fig. 8) would be used rather than the reduced values. In this study, the vertical motion was scaled by 0.2 so that the  $x_b$ - $y_b$  envelope (fig. 2) remained large and the performance in the longitudinal channel would be as good as possible. An example of the performance in the longitudinal channel for sinusoidal inputs with an amplitude typical of pilot inputs ( $\gamma_c = 3^\circ$ ) is presented in figure 19. In the longitudinal channel the modified washout shows an improvement in amplitude ratio for low-frequency inputs that is comparable to the vertical channel. In addition, the amplitude ratio of the longitudinal chan-

nel exhibits a more conventional variation with forcing frequency than was premitted in the vertical channel.

The modified washout logic with reduced filter parameters was believed by the pilots to be the best of all the variations investigated for performing the landing-approach task in low-level turbulence (see fig. 20). In addition, it was the only variation that could be detected as being different from the washout-with-braking logic. It is difficult to make any comparisons between the modified washout logic (fig. 20) and the washout-with-braking logic (fig. 16) in typical piloted flights because of the necessary low-level turbulence with an rms level of 0.3 m/sec (1 ft/sec). In figure 20, for example, the pilot commanded flight-path angle  $\gamma_c$  changes at approximately 11, 15, 27, 41, and 51 seconds. It would appear that the pilot cannot tell the difference between a vertical acceleration  $a_z$  due to turbulence and one due to a control input using the magnitude of the sensed acceleration as the only cue. The fact that the pilot is favorably influenced by the accelerations resulting from his control inputs, therefore, seems to be because he expects to feel something whenever he makes a control input. Between control inputs the pilot accepts any accelerations he feels as being due to turbulence and more or less ignores them.

#### CONCLUDING REMARKS

A motion-constraint logic for moving-base simulators has been developed that is a modification to the linear second-order filters generally employed in the more conventional approaches. In the modified washout logic, the filter parameters are not constant but vary with the instantaneous motion-base position to increase the constraint as the system approaches the positional limits. The primary advantage of the modified washout logic stems from the fact that the basic filter parameters can be chosen so that the resulting amplitude ratios are improved in the low-frequency regime where the pilot's motion-sensing abilities are best. This improvement is achieved without a significant degradation in phase angle. In addition, accelerations larger than originally expected are successfully limited. Thus, the modified washout logic can have the basic filter parameters scaled for a particular task, and the few inadvertent acceleration spikes caused by a pilot not yet up on the learning curve will not destroy the run.

For the externally blown flap STOL landing task using decoupled controls employed in the current investigation, the pilots were unable to tell much difference between the modified washout and the washout-with-braking constraints. In fact, the pilots slightly preferred the modified washout even though a simple conservative estimate of the base

position limits was employed while the washout-with-braking logic used a fairly sophisticated prediction technique to estimate the position limits.

Langley Research Center,  
National Aeronautics and Space Administration,  
Hampton, Va., October 3, 1974.



## REFERENCES

1. Bergeron, Hugh P.; and Adams, James J.: Measured Transfer Functions of Pilots During Two-Axis Tasks With Motion. NASA TN D-2177, 1964.
2. Morris, W. B.; McCormick, R. L.; and Sinacori, J. B.: Moving-Base Simulator Study of an All-Mechanical Control System for VTOL Aircraft. *J. Aircraft*, vol. 1, no. 1, Jan.-Feb. 1964, pp. 41-45.
3. Perry, D. H.; Warton, L. H.; and Welbourn, C. E.: A Flight Simulator for Research Into Aircraft Handling Characteristics. R. & M. No. 3566, Brit. A.R.C., 1969.
4. Schmidt, Stanley F.; and Conrad, Bjorn: Motion Drive Signals for Piloted Flight Simulators. NASA CR-1601, 1970.
5. Schmidt, Stanley F.; and Conrad, Bjorn: A Study of Techniques for Calculating Motion Drive Signals for Flight Simulators. Rep. No. 71-28, Analytical Mechanics Associates, Inc., July 1971. (Available as NASA CR-114345.)
6. Parrish, Russell V.; Dieudonne, James E.; and Martin, Dennis J., Jr.: Motion Software for a Synergistic Six-Degree-of-Freedom Motion Base. NASA TN D-7350, 1973.
7. Dieudonne, James E.; Parrish, Russell V.; and Bardusch, Richard E.: An Actuator Extension Transformation for a Motion Simulator and an Inverse Transformation Applying Newton-Raphson's Method. NASA TN D-7067, 1972.
8. Gallagher, J. T.: Requirements on Simulators Used in Handling Qualities Research. AIAA Paper No. 70-353, Mar. 1970.
9. Sinacori, J. B.: Application of the Northrop Rotational Simulator to Helicopters and V/STOL Aircraft (User's Guide). USAAVLABS Tech. Rep. 70-26, U.S. Army, May 1970. (Available from DDC as AD 873 037.)
10. Miller, G. Kimball, Jr.; Deal, Perry L.; and Champine, Robert A.: Fixed-Base Simulation Study of Decoupled Controls During Approach and Landing of a STOL Transport Airplane. NASA TN D-7363, 1974.
11. Friedland, Bernard; Ling, Chong-Kuan; and Hutton, Maurice F.: Quasi-Optimum Design of Six Degree of Freedom Moving Base Simulator Control System. NASA CR-2312, 1973.

TABLE I.- LANGLEY VMS PERFORMANCE LIMITS FOR EACH INDEPENDENT DEGREE OF FREEDOM FOR A NEUTRAL POINT 2.58 m (8.46 ft) ABOVE THE FLOOR

Degree of freedom	Performance limits		
	Position	Velocity	Acceleration
Longitudinal	Fore 1.245 m (4.08 ft)	$\pm 0.610$ m/sec (2.00 ft/sec)	$\pm 0.6g$
	Aft 1.219 m (4.00 ft)		
Lateral	Left 1.219 m (4.00 ft)	$\pm 0.610$ m/sec (2.00 ft/sec)	$\pm 0.6g$
	Right 1.219 m (4.00 ft)		
Vertical	Up 0.991 m (3.25 ft)	$\pm 0.610$ m/sec (2.00 ft/sec)	$\pm 0.6g$
	Down 0.762 m (2.50 ft)		
Yaw	$\pm 32$ deg	$\pm 15$ deg/sec	$\pm 50$ deg/sec <sup>2</sup>
Pitch	+30 deg	$\pm 15$ deg/sec	$\pm 50$ deg/sec <sup>2</sup>
	-20 deg		
Roll	$\pm 22$ deg	$\pm 15$ deg/sec	$\pm 50$ deg/sec <sup>2</sup>

TABLE II. - WASHOUT-PARAMETER VALUES USED IN THE WASHOUT-WITH-BRAKING LOGIC

[Variables defined in reference 6]

Variable	Value in SI units	Program value
$k_{z,1}$ . . . . .	0.2	0.2
$\xi_{z,1}$ . . . . .	0.7	0.7
$\omega_{n,z,1}$ , rad/sec . . . . .	0.1	0.1
$k_{z,2}$ . . . . .	1.0	1.0
$k_{p,T,1}$ , per m (per ft) . . .	0.013	0.004
$k_{p,T,2}$ , sec . . . . .	3.8	3.8
$k_{p,T,3}$ , per sec . . . . .	0.05	0.05
$k_{q,T,1}$ , per m (per ft) . . .	0.013	0.004
$k_{q,T,2}$ , sec . . . . .	3.8	3.8
$k_{q,T,3}$ , per sec . . . . .	0.05	0.05
$k_{r,1}$ , per m (per ft) . . . .	0.0131	0.004
$k_{r,2}$ , sec . . . . .	3.8	3.8
$k_{r,3}$ , per sec . . . . .	0.05	0.05
$a_1$ , rad/sec . . . . .	1.414	1.414
$a_2$ , rad/sec . . . . .	2.1	2.1
$a_3$ , rad/sec . . . . .	2.1	2.1
$b_1$ , rad/sec . . . . .	1.0	1.0
$b_2$ , rad/sec . . . . .	2.25	2.25
$b_3$ , rad/sec . . . . .	2.25	2.25
$\ddot{x}_l$ , m/sec <sup>2</sup> (ft/sec <sup>2</sup> ) . . . .	5.8840	19.3044
$\ddot{y}_l$ , m/sec <sup>2</sup> (ft/sec <sup>2</sup> ) . . . .	5.8840	19.3044
$\ddot{z}_l$ , m/sec <sup>2</sup> (ft/sec <sup>2</sup> ) . . . .	7.8453	25.7392
$A_1$ , sec <sup>2</sup> . . . . .	0.007	0.007
$A_2$ , sec <sup>2</sup> . . . . .	0.007	0.007
$A_3$ , sec <sup>2</sup> . . . . .	0.007	0.007

Variable	Value in SI units	Program value
$B_1$ , sec . . . . .	0.15	0.15
$B_2$ , sec . . . . .	0.15	0.15
$B_3$ , sec . . . . .	0.133	0.133
$k_{\psi,l}$ , sec . . . . .	0.15	0.15
$k_{\theta,l}$ , sec . . . . .	0.15	0.15
$k_{\phi,l}$ , sec . . . . .	0.15	0.15
$k_p$ . . . . .	0.5	0.5
$k_q$ . . . . .	1.0	1.0
$k_r$ . . . . .	1.0	1.0
$C_1$ , per sec . . . . .	0.5	0.5
$C_2$ , per sec . . . . .	0.2	0.2
$C_3$ , per sec . . . . .	0.5	0.5
$k_{\theta,1}$ . . . . .	1.0	1.0
$k_{\theta,2}$ . . . . .	0.04	0.04
$\xi_{\theta}$ . . . . .	0.028	0.028
$\omega_{n,\theta}$ , rad/sec . . . . .	1.0	1.0
$k_{\phi,1}$ . . . . .	0.5	0.5
$k_{\phi,2}$ . . . . .	0.04	0.04
$\xi_{\phi}$ . . . . .	0.028	0.028
$\omega_{n,\phi}$ , rad/sec . . . . .	1.0	1.0
$z_{\text{neut}}$ , m (ft) . . . . .	0.6487	2.128
$V_l$ , m/sec (ft/sec) . . . . .	0.3048	1.0
$x_{LF}$ . . . . .	2.5	2.5
$y_{LF}$ . . . . .	2.5	2.5
$z_{LF}$ . . . . .	3.0	3.0



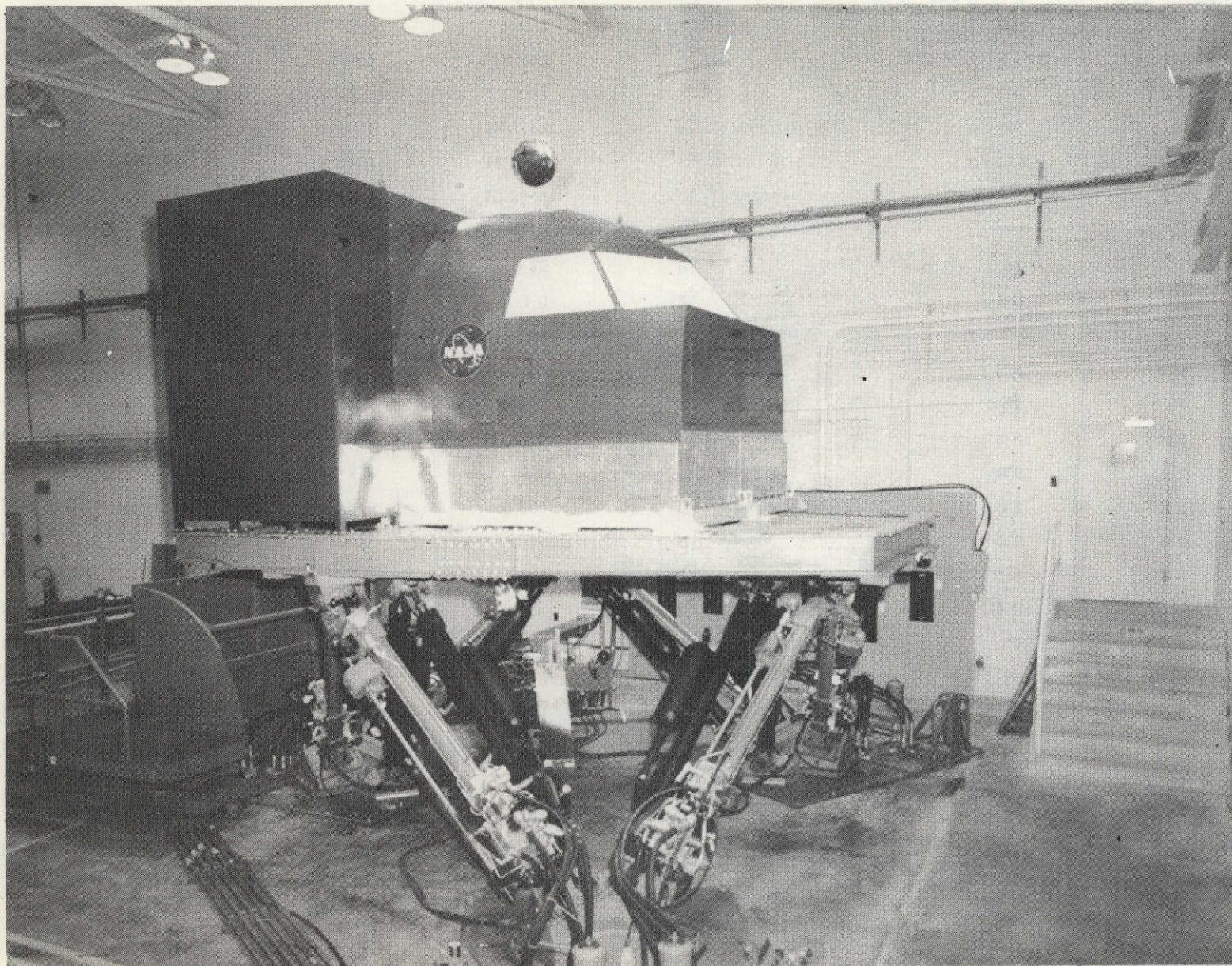


Figure 1.- The Langley visual-motion simulator (VMS).

L-72-3233



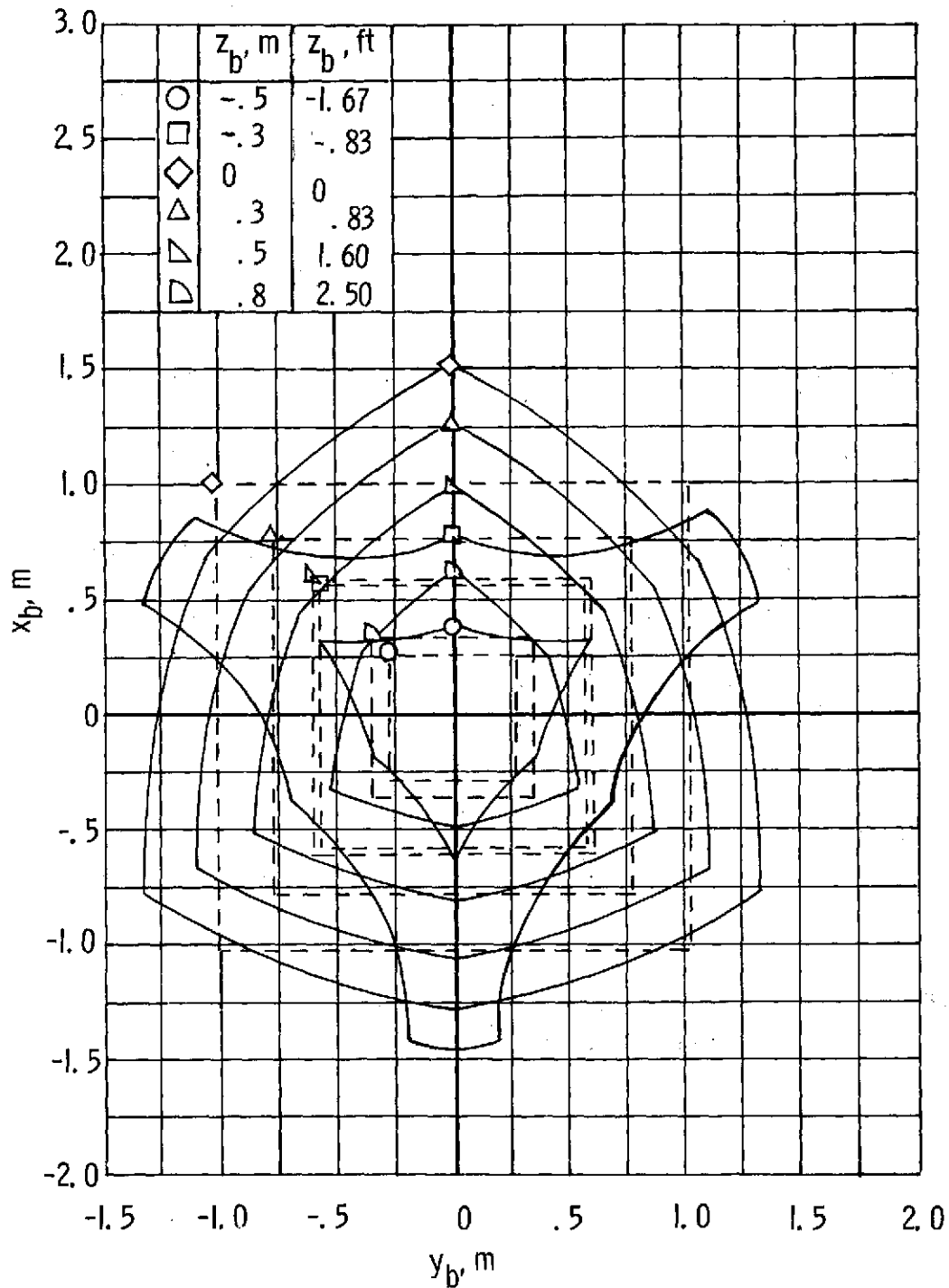


Figure 2.- Motion-base operational envelope in horizontal ( $x_b$ - $y_b$ ) plane as a function of its vertical position ( $z_b$ ). (Dashed lines denote simplified envelope assumed for analysis.)

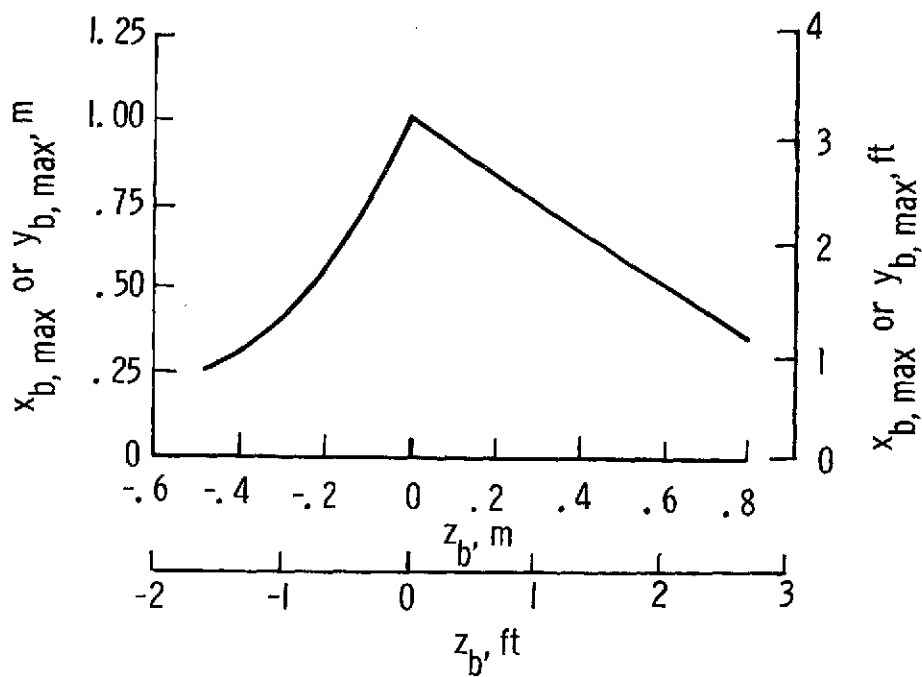


Figure 3.- Maximum permissible displacements in horizontal plane as functions of vertical position of motion base.

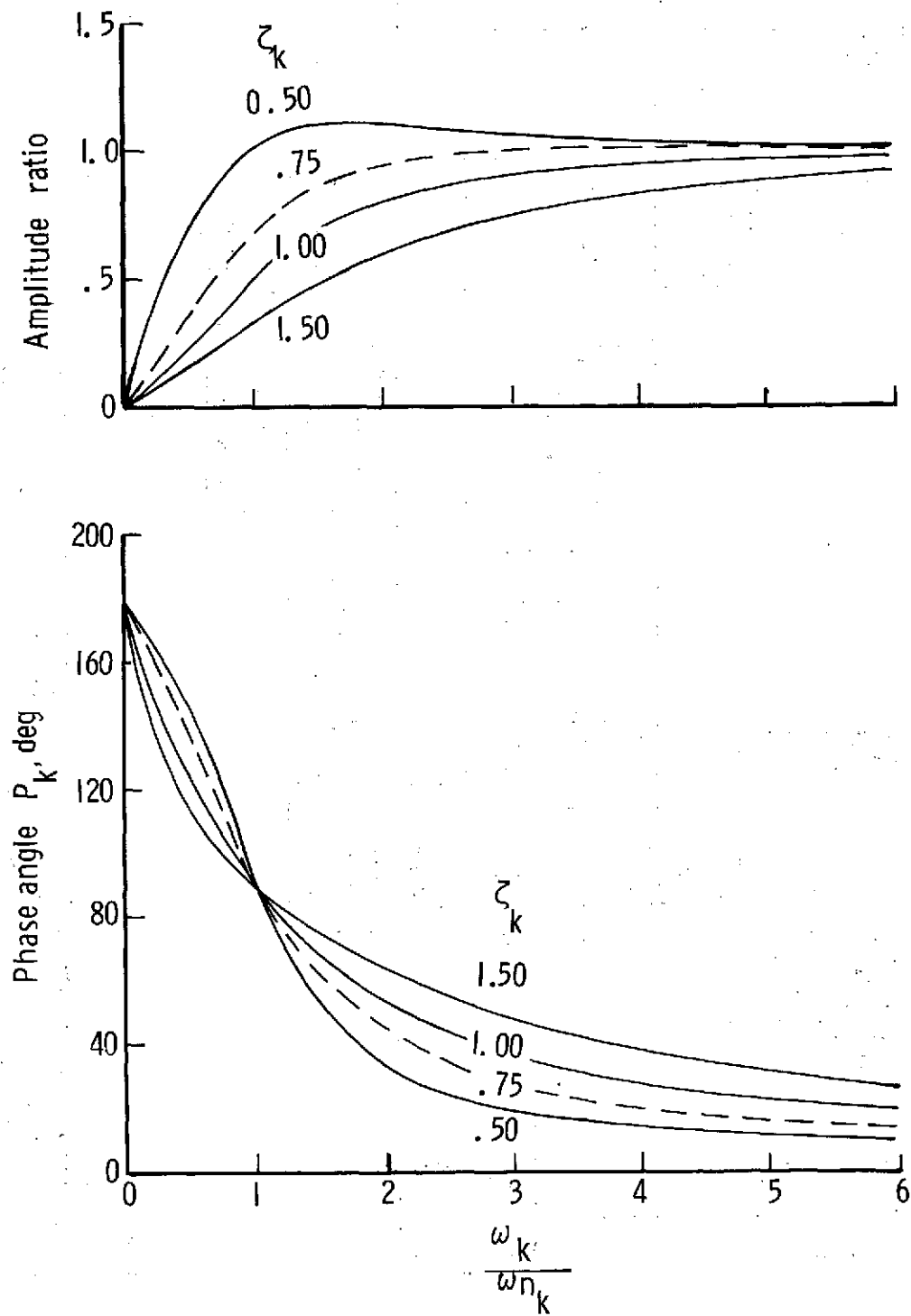
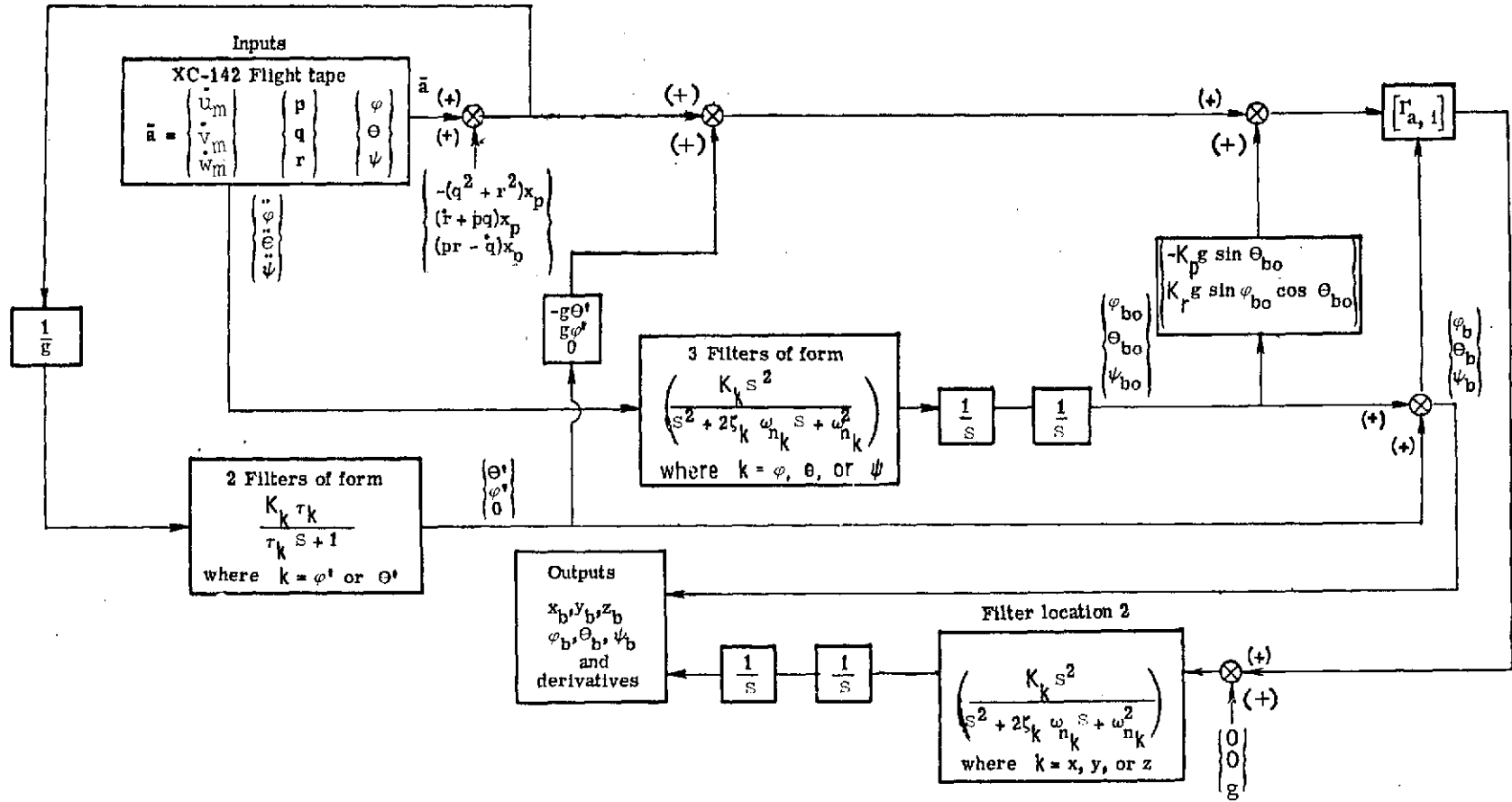


Figure 4.- Second-order linear filter dynamics.  $K_k = 1.0$ .



where

$$[r_{a, i}] = \begin{bmatrix} (\cos \Theta_b \cos \psi_b) & (\sin \varphi_b \sin \Theta_b \cos \psi_b - \cos \varphi_b \sin \psi_b) & (\cos \varphi_b \sin \Theta_b \cos \psi_b + \sin \varphi_b \sin \psi_b) \\ (\cos \Theta_b \sin \psi_b) & (\sin \varphi_b \sin \Theta_b \sin \psi_b + \cos \varphi_b \cos \psi_b) & (\cos \varphi_b \sin \Theta_b \sin \psi_b - \sin \varphi_b \cos \psi_b) \\ (-\sin \Theta_b) & (\sin \varphi_b \cos \Theta_b) & (\cos \varphi_b \cos \Theta_b) \end{bmatrix}$$

Figure 5.- Basic constraint logic.



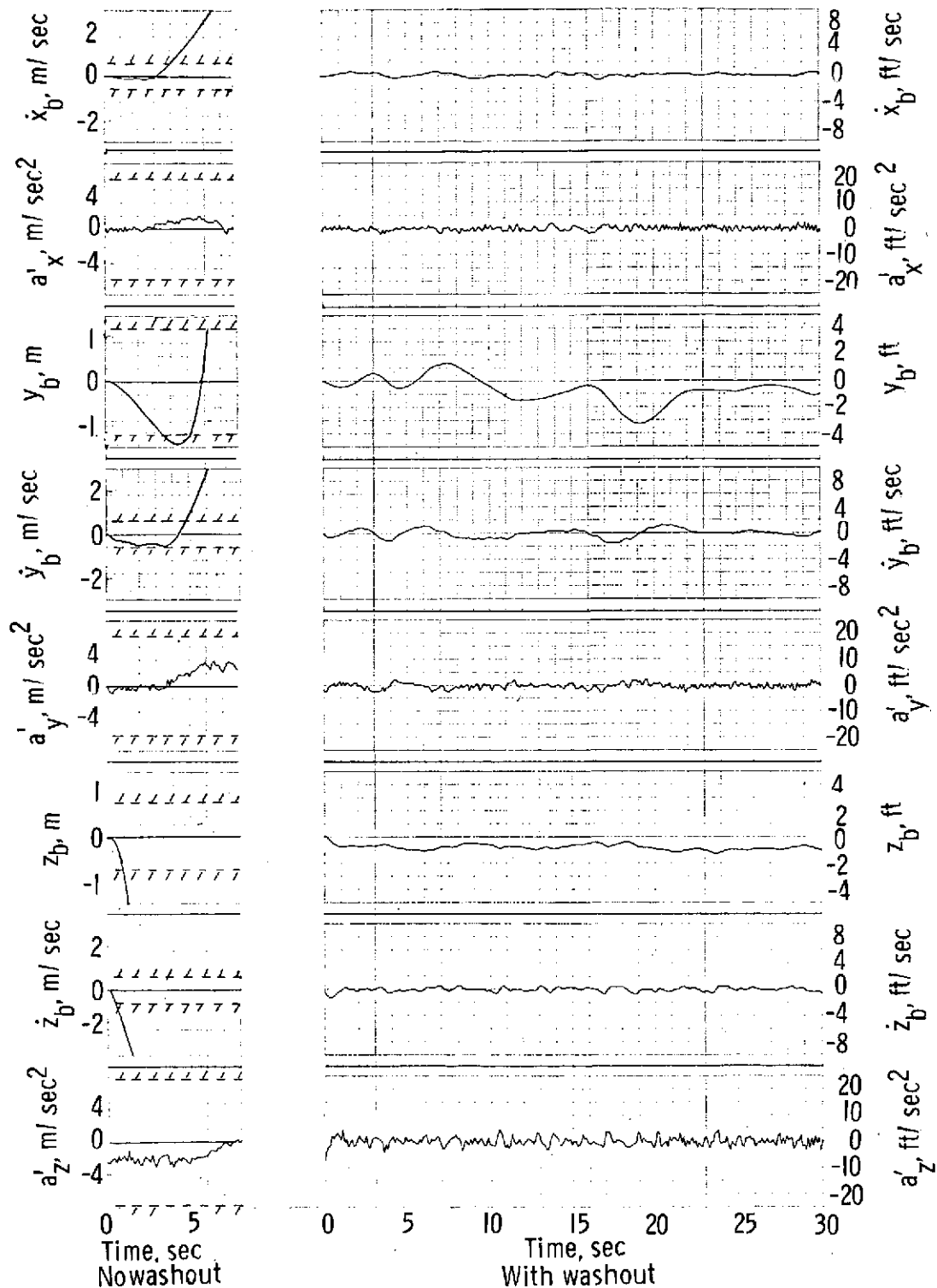


Figure 6.- Response of motion base to "wind-up turn" flight tape with conventional washout and without washout. (Single-degree-of-freedom base limits denoted by hatched lines.)

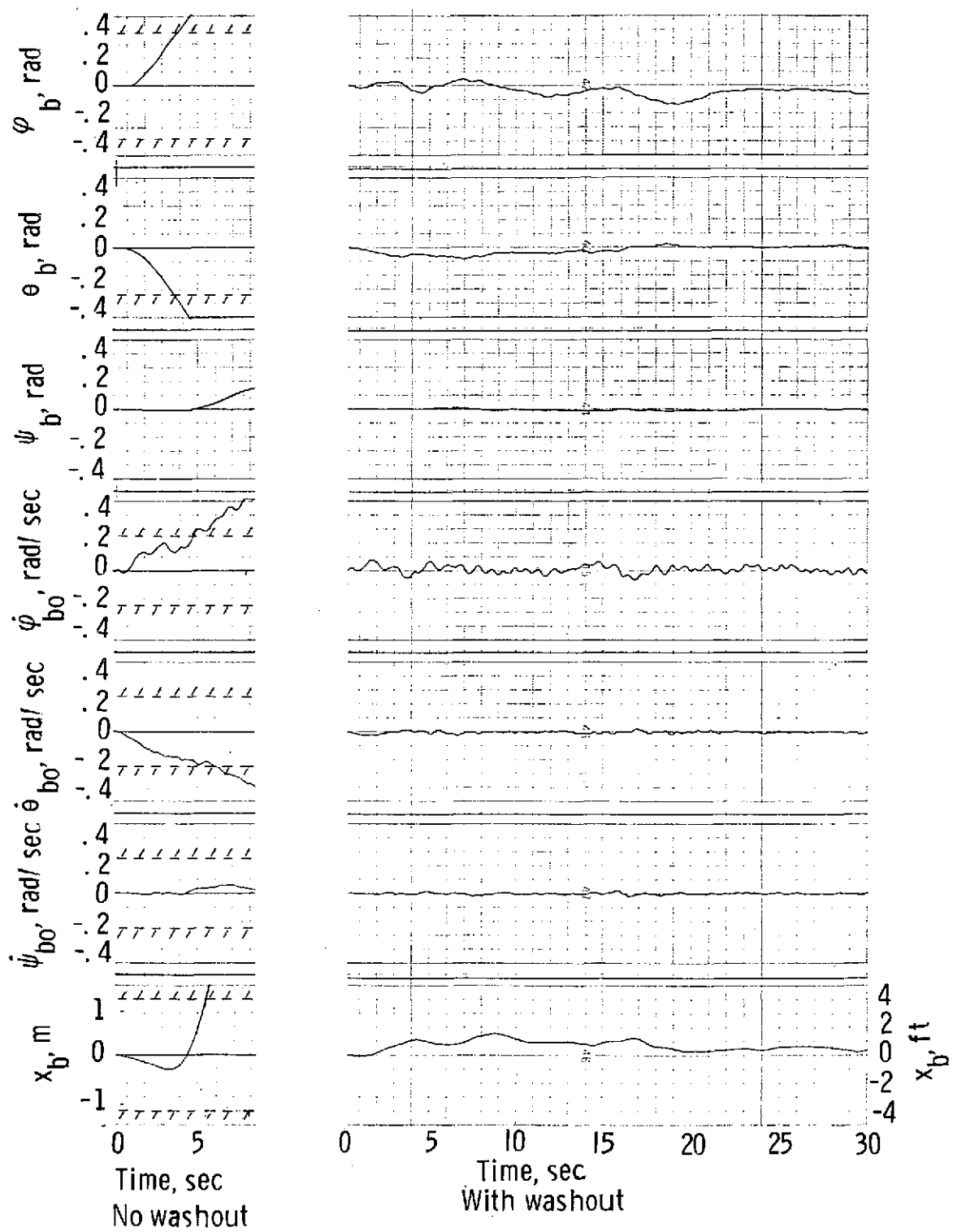


Figure 6.- Concluded.

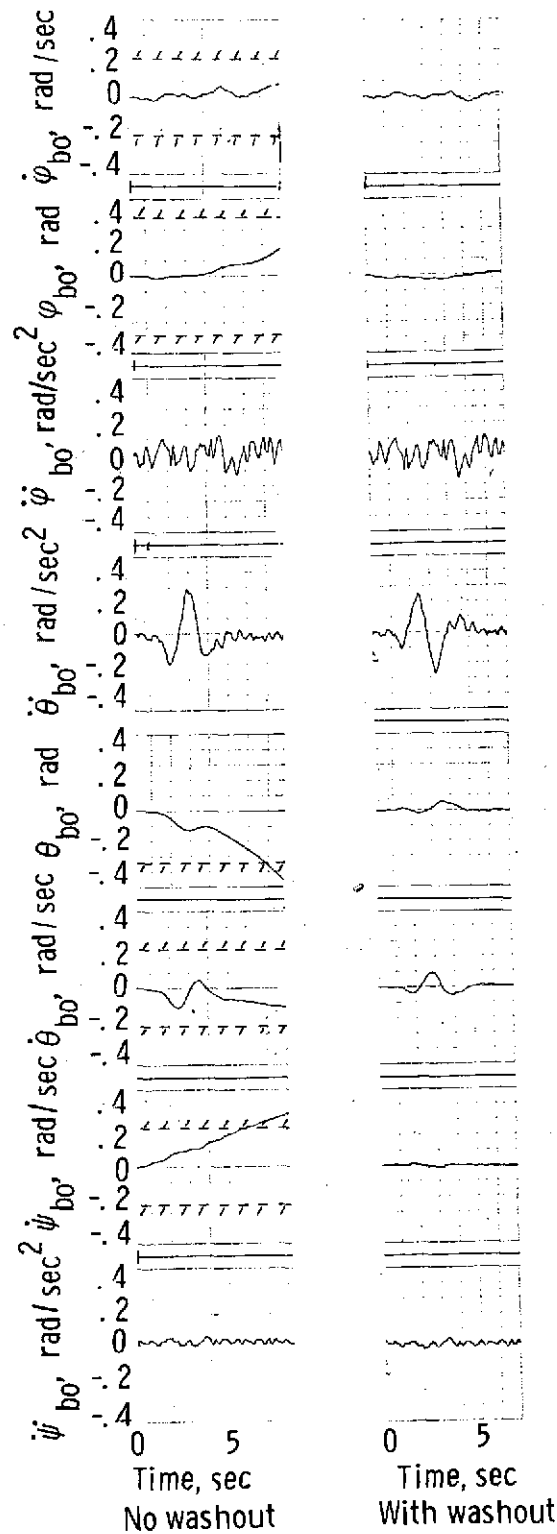


Figure 7.- Comparison of conventional washout and no washout for pitch doublet. (Base limits denoted by hatched lines.)

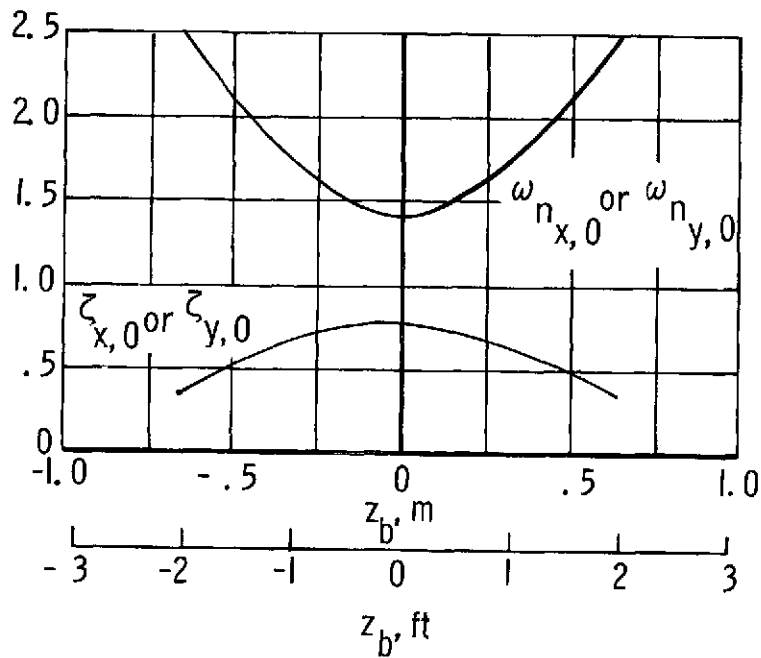
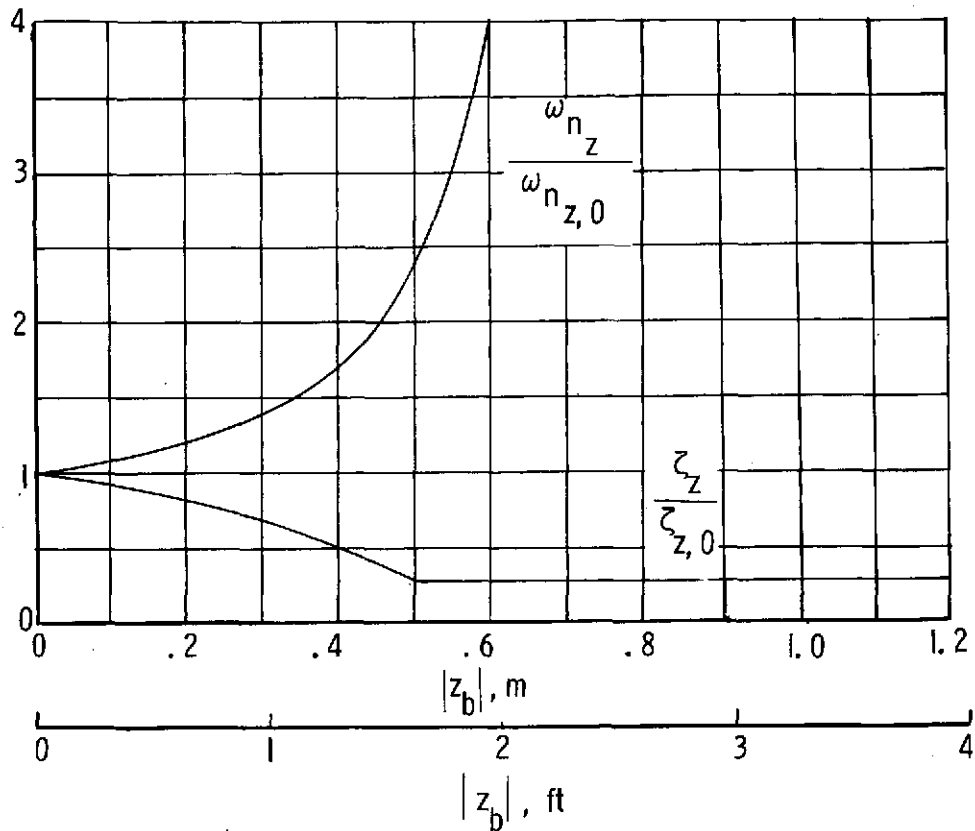
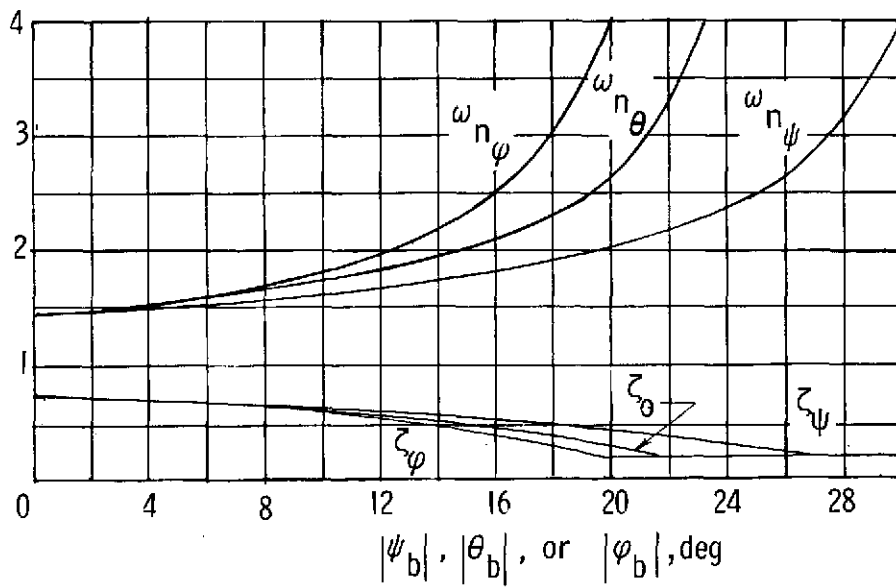


Figure 8.- Base-line values of washout parameters for the  $x_b$  and  $y_b$  axes as functions of the vertical base displacement  $z_b$  from the null position. ( $\omega_{n_z,0} = 3.1$  and  $\zeta_{z,0} = 0.50$ .)



(a) Vertical channel.



(b) Angular channels.

Figure 9.- Modified washout parameters for the vertical and angular degrees of freedom as functions of the instantaneous base positions.

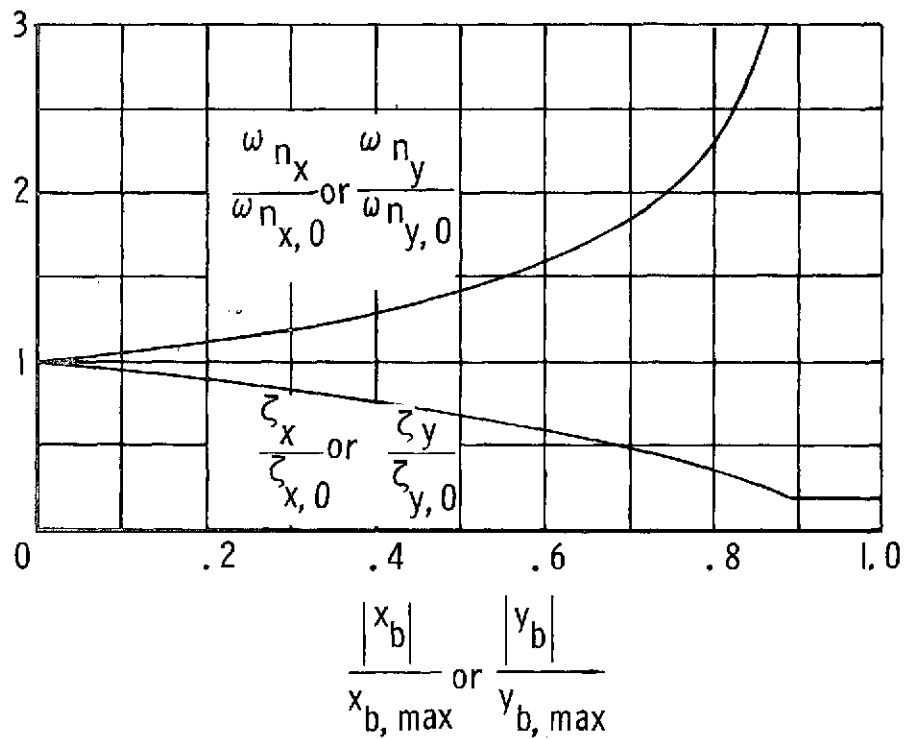


Figure 10.- Modified washout parameters for the longitudinal and lateral axes as functions of the instantaneous base positions.

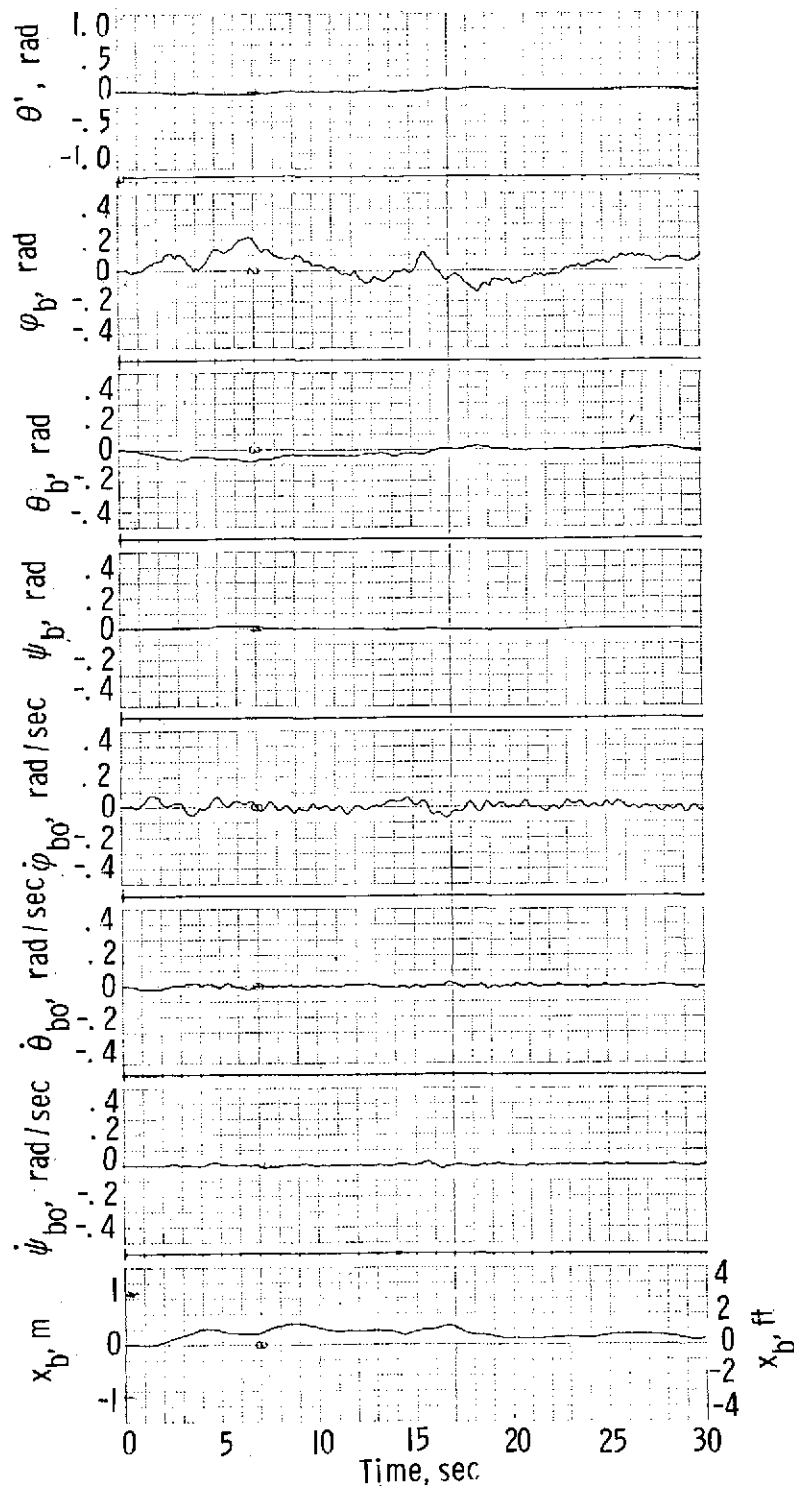


Figure 11.- Wind-up turn flight tape with conventional washout and with cockpit 30.48 meters (100 ft) forward of airplane center of gravity.

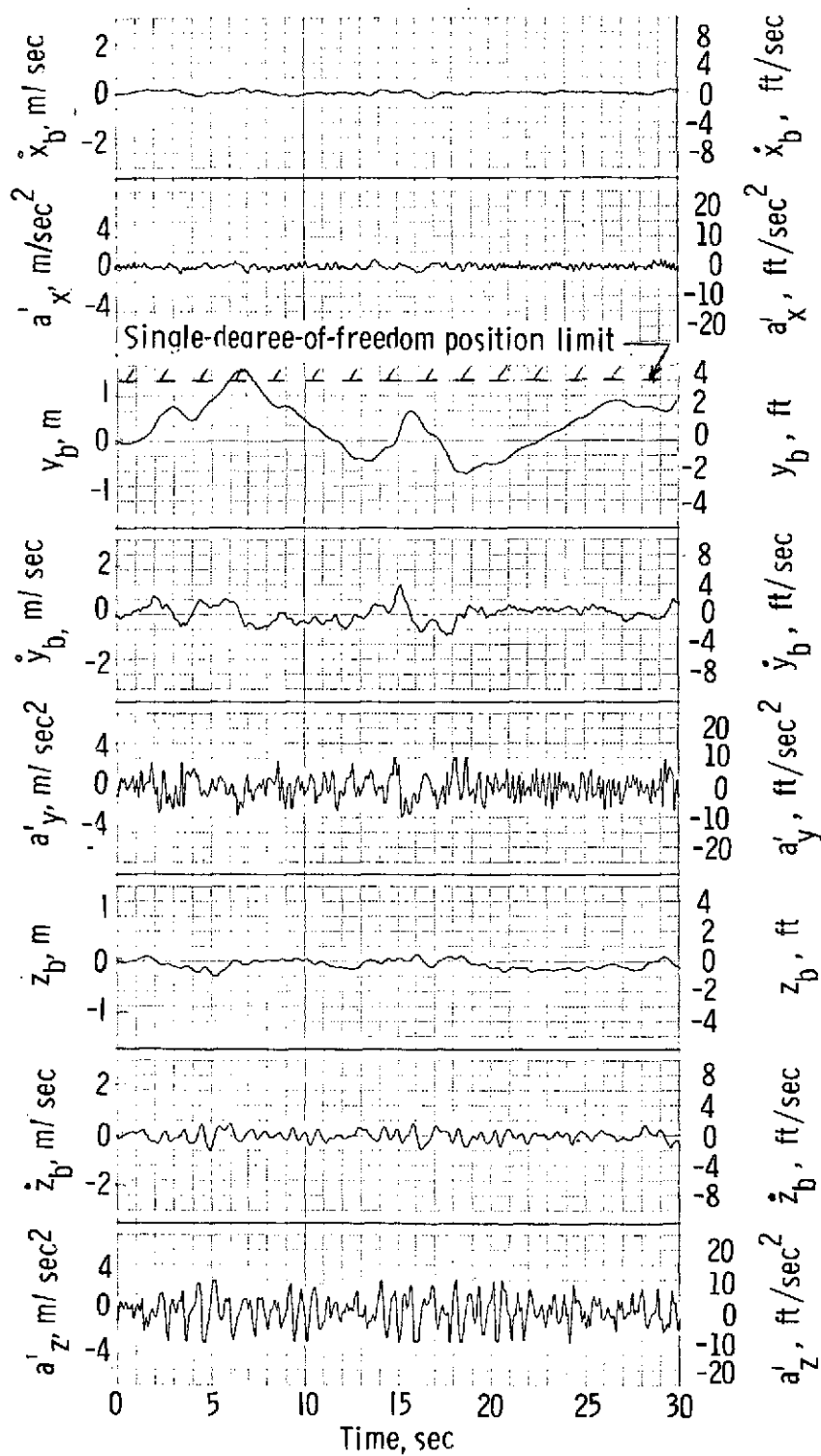


Figure 11.- Concluded.



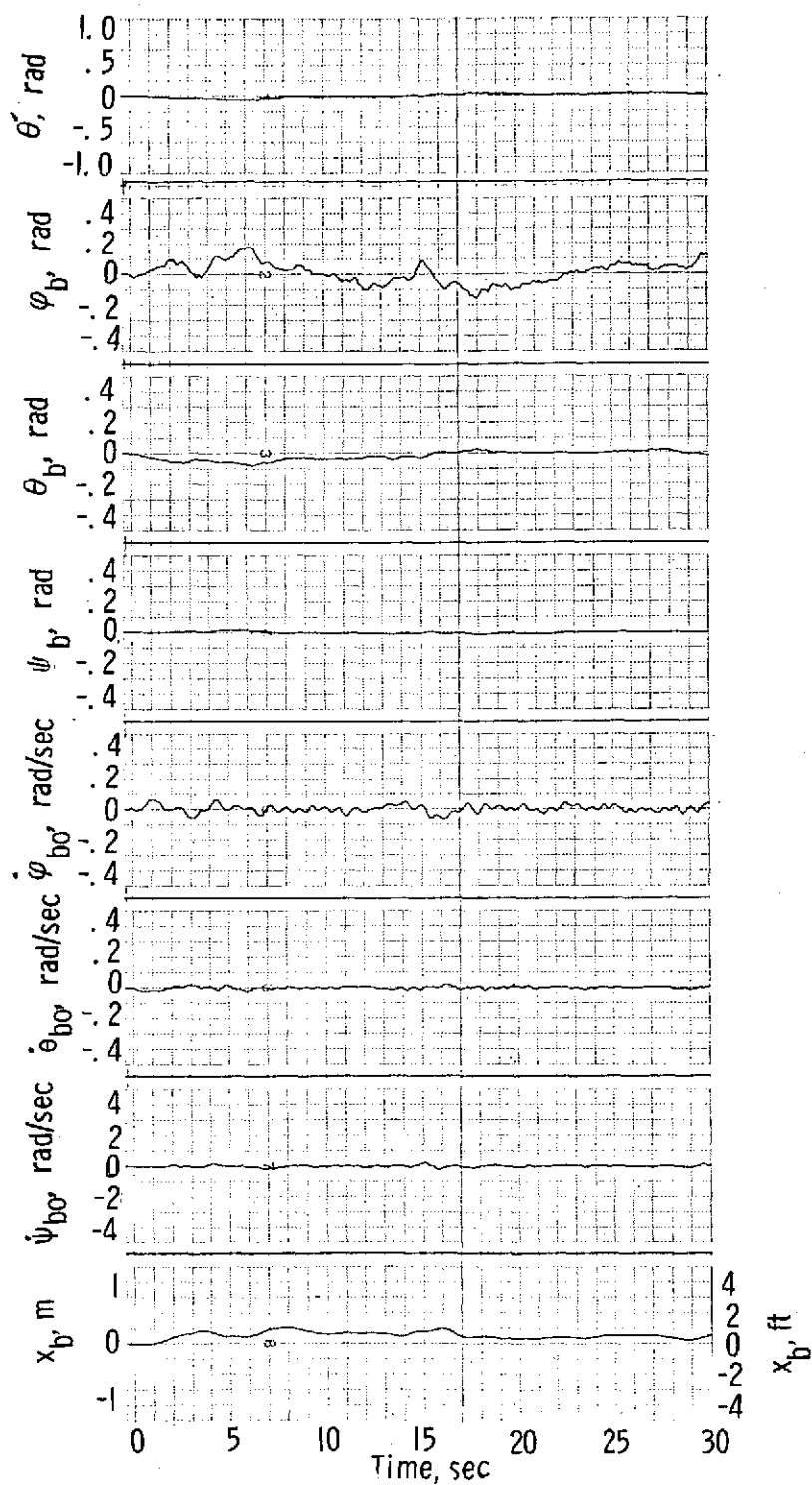


Figure 12.- Wind-up turn flight tape with modified washout and with cockpit 30.48 meters (100 ft) forward of airplane center of gravity.

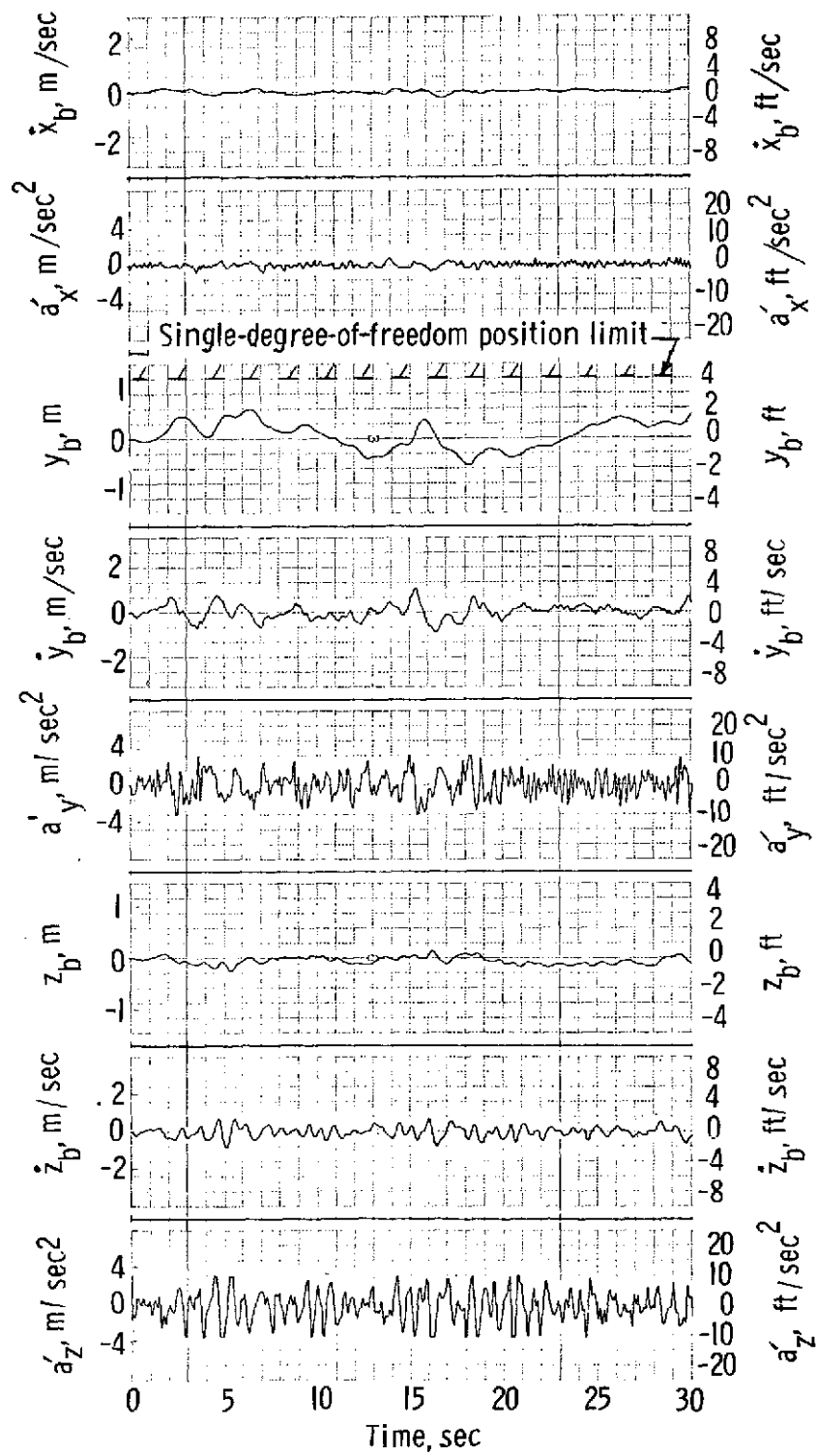


Figure 12.- Concluded.

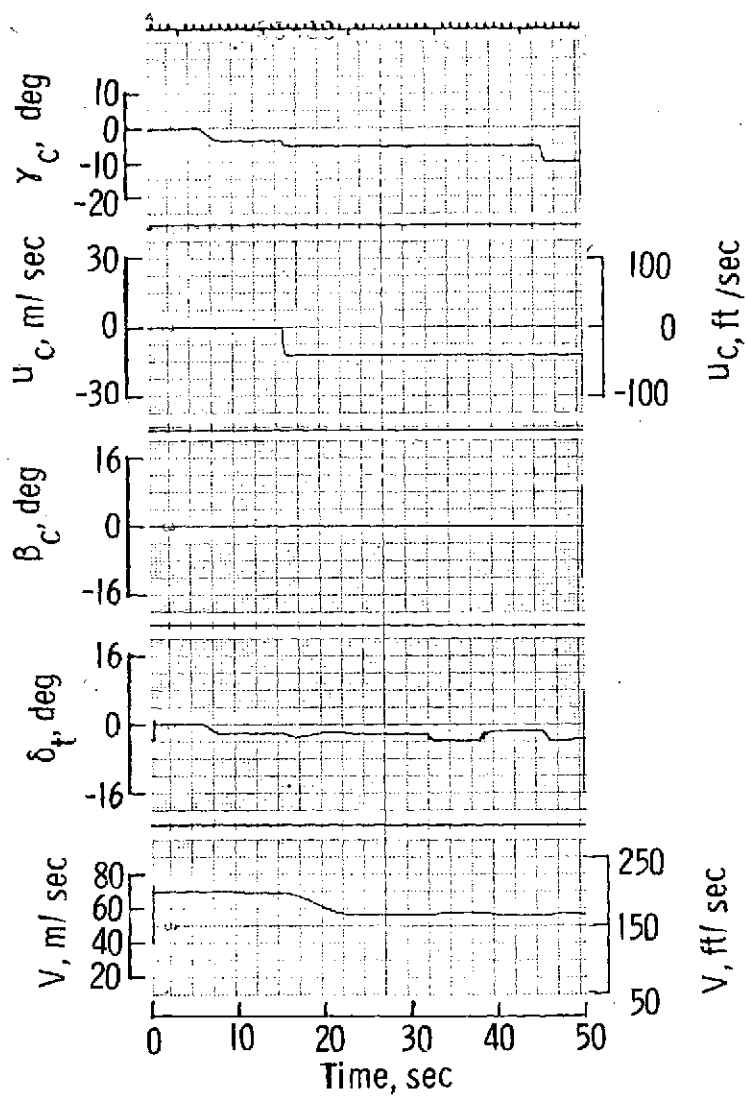


Figure 13.- Response of externally blown flap STOL decoupled longitudinal control system.

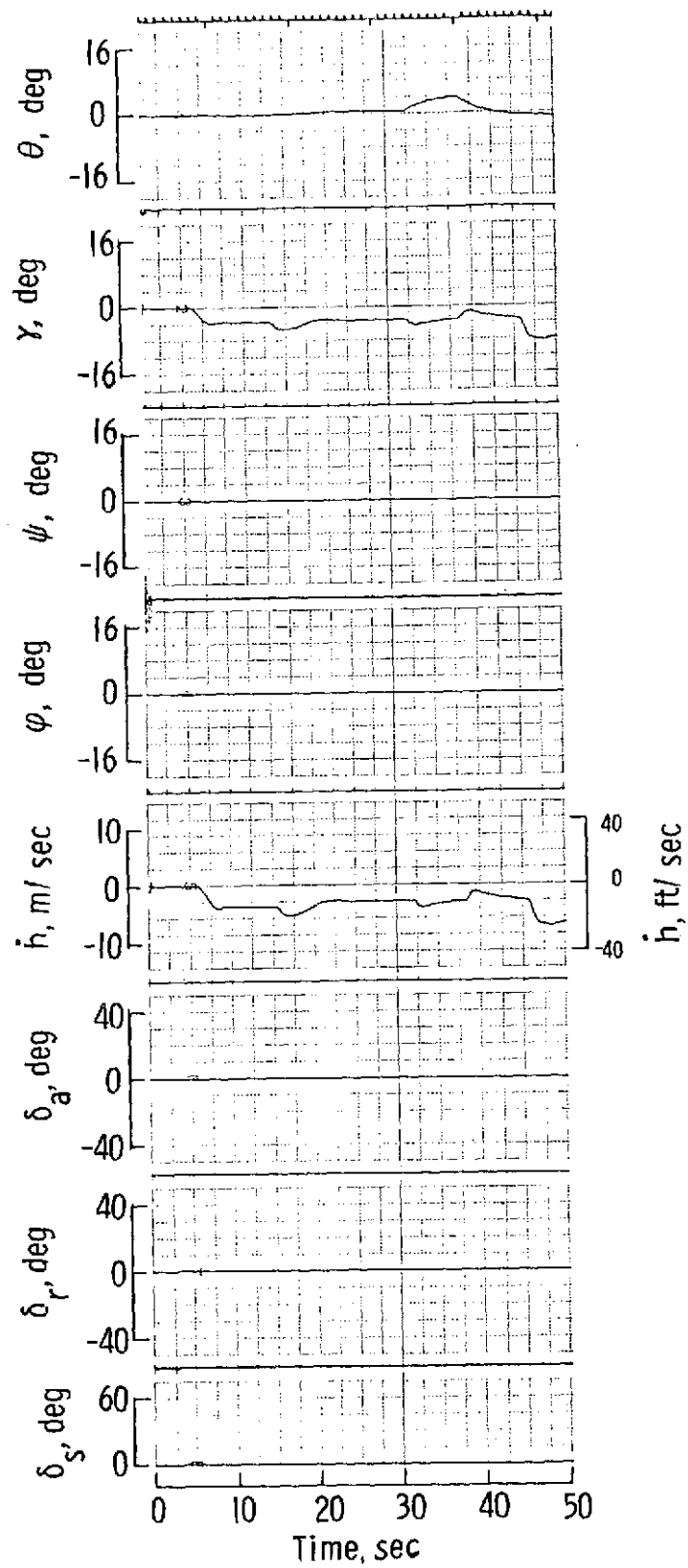


Figure 13.- Continued.

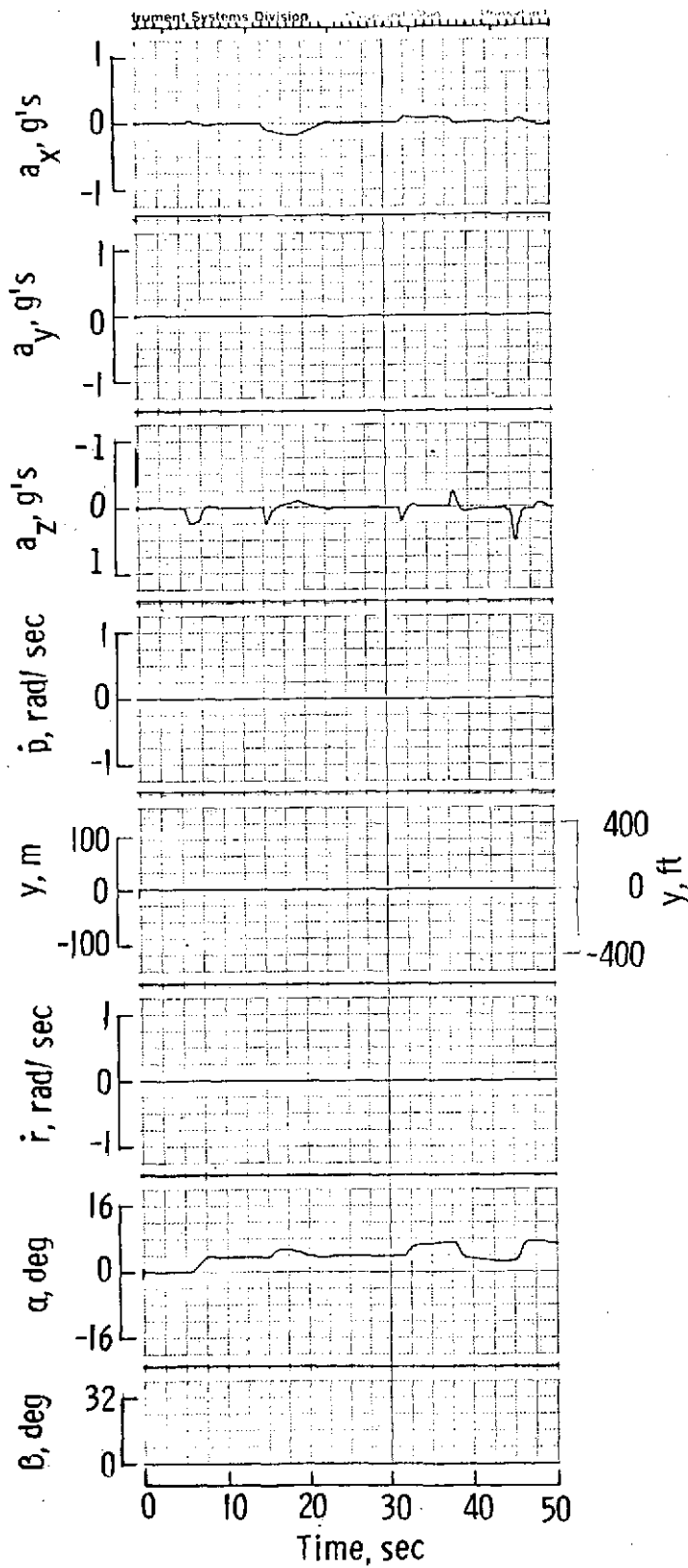


Figure 13. - Concluded.

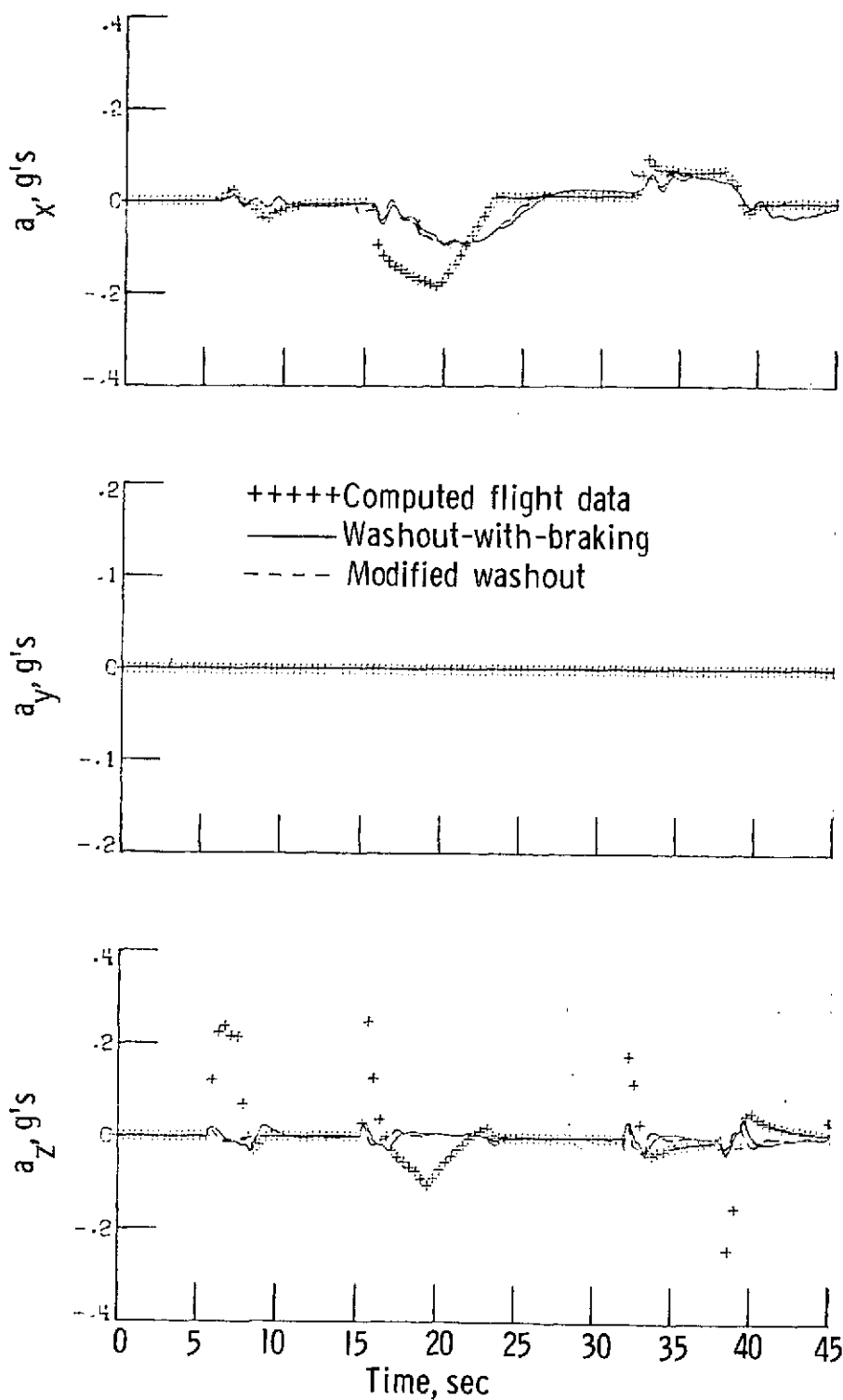


Figure 14.- Computed motion-base response to dynamic response check for externally blown flap STOL transport with decoupled longitudinal controls.

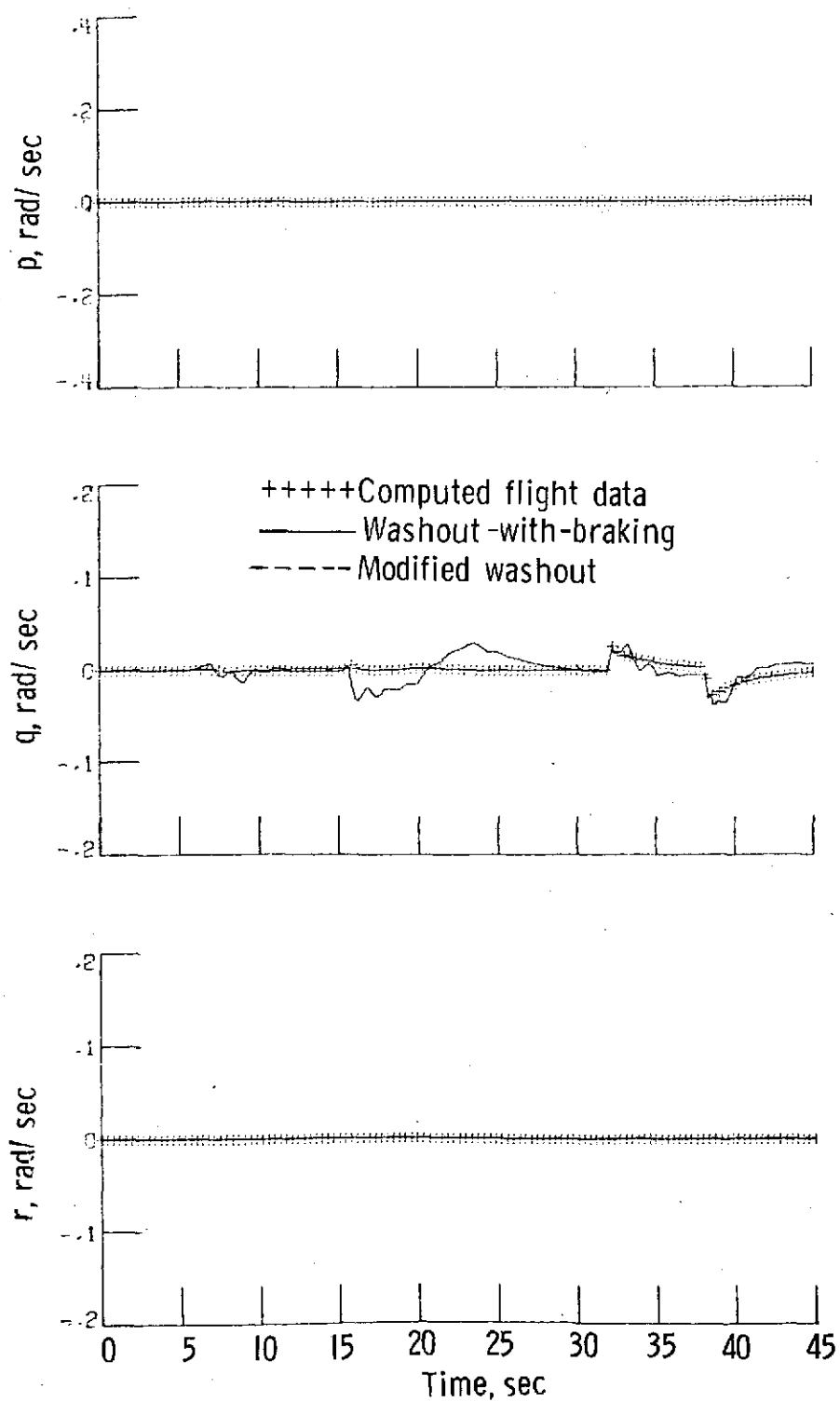


Figure 14.- Continued.

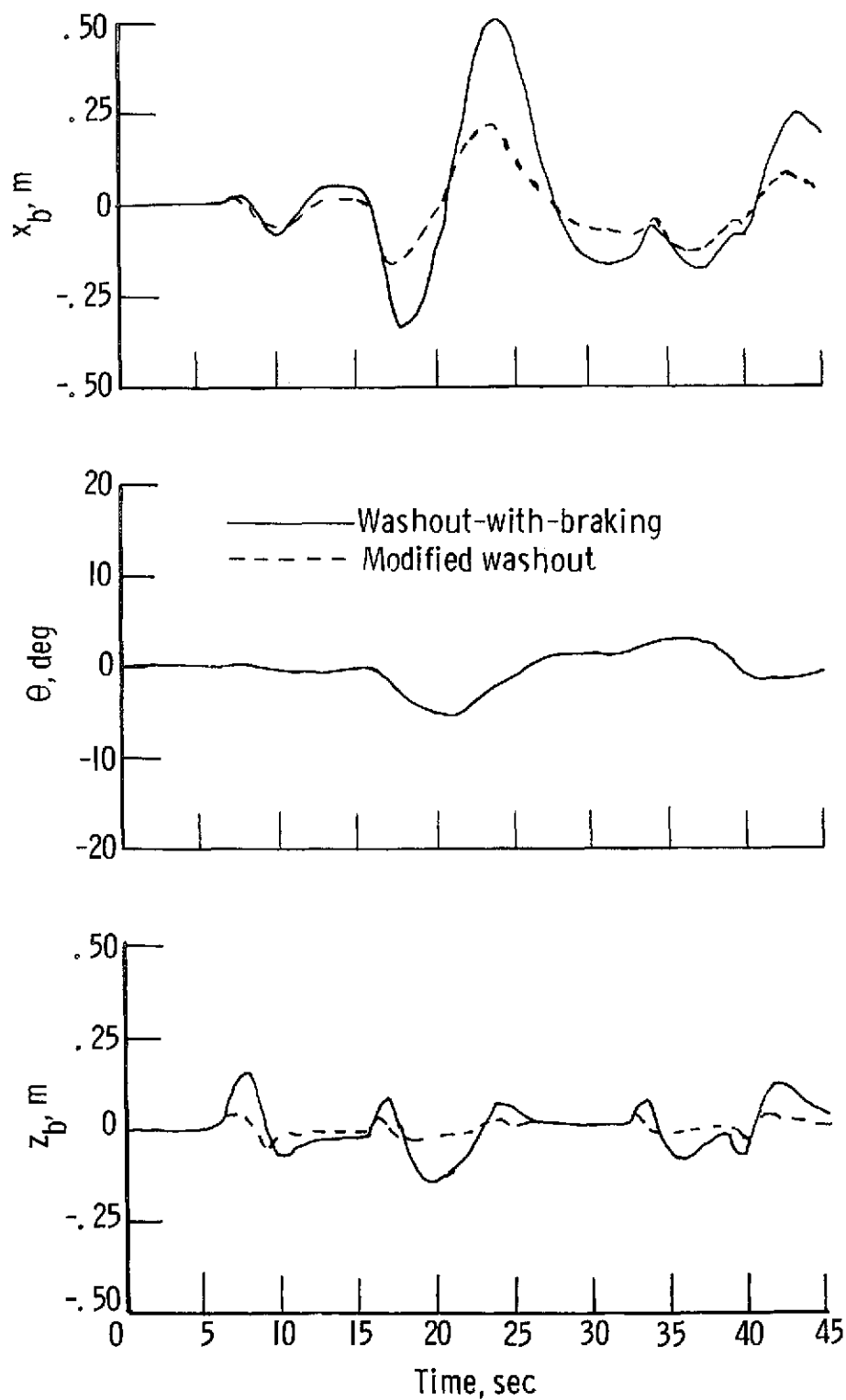


Figure 14.- Continued.



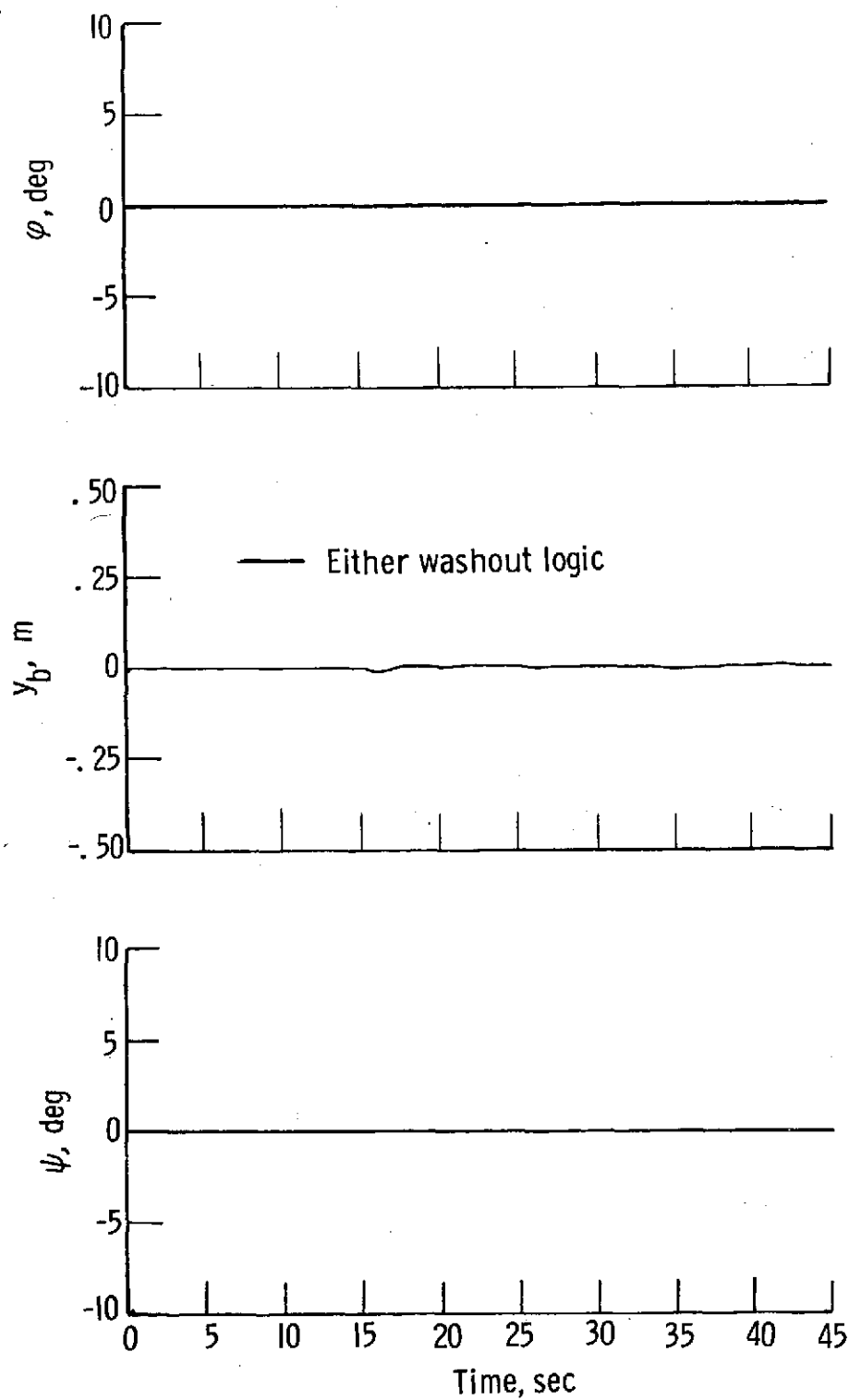


Figure 14.- Concluded.

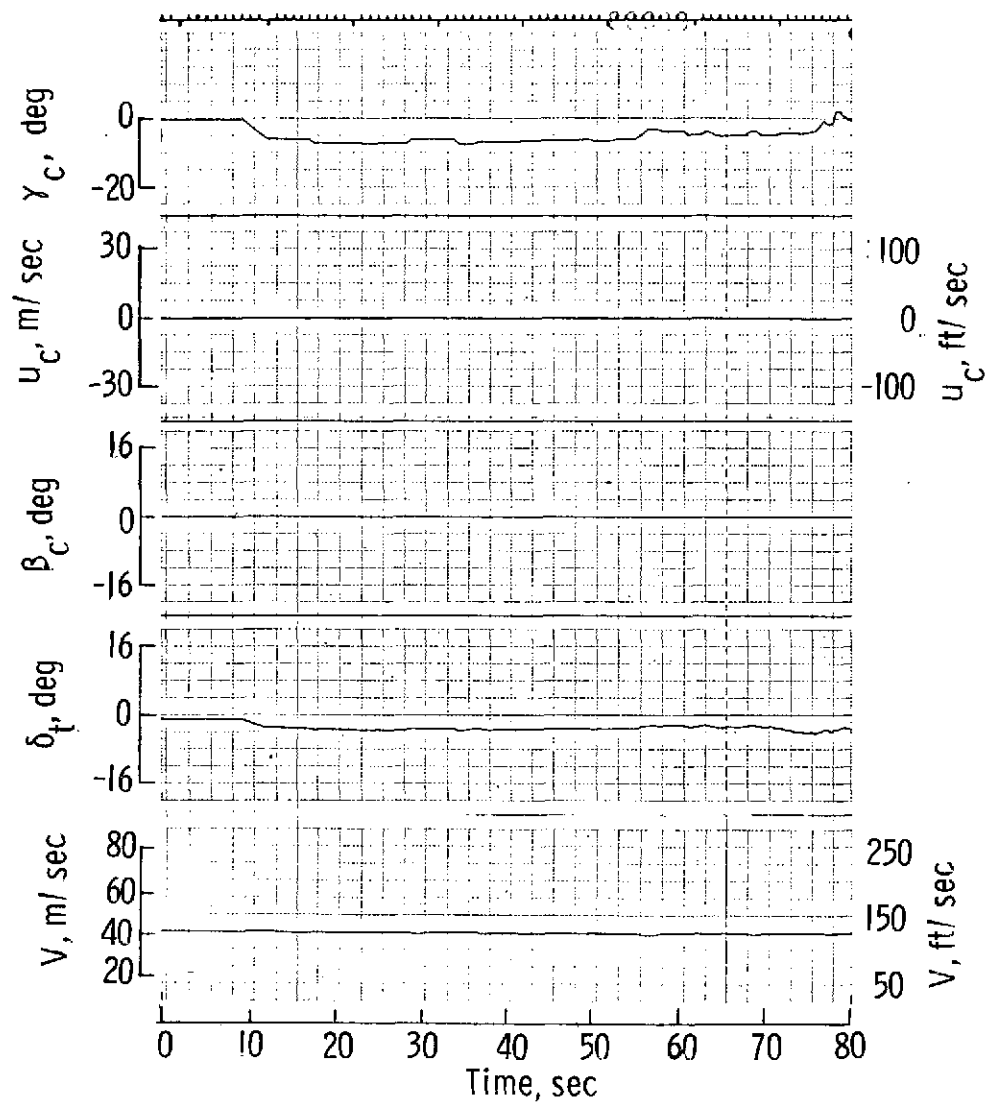


Figure 15.- Typical landing approach made in low-level turbulence.

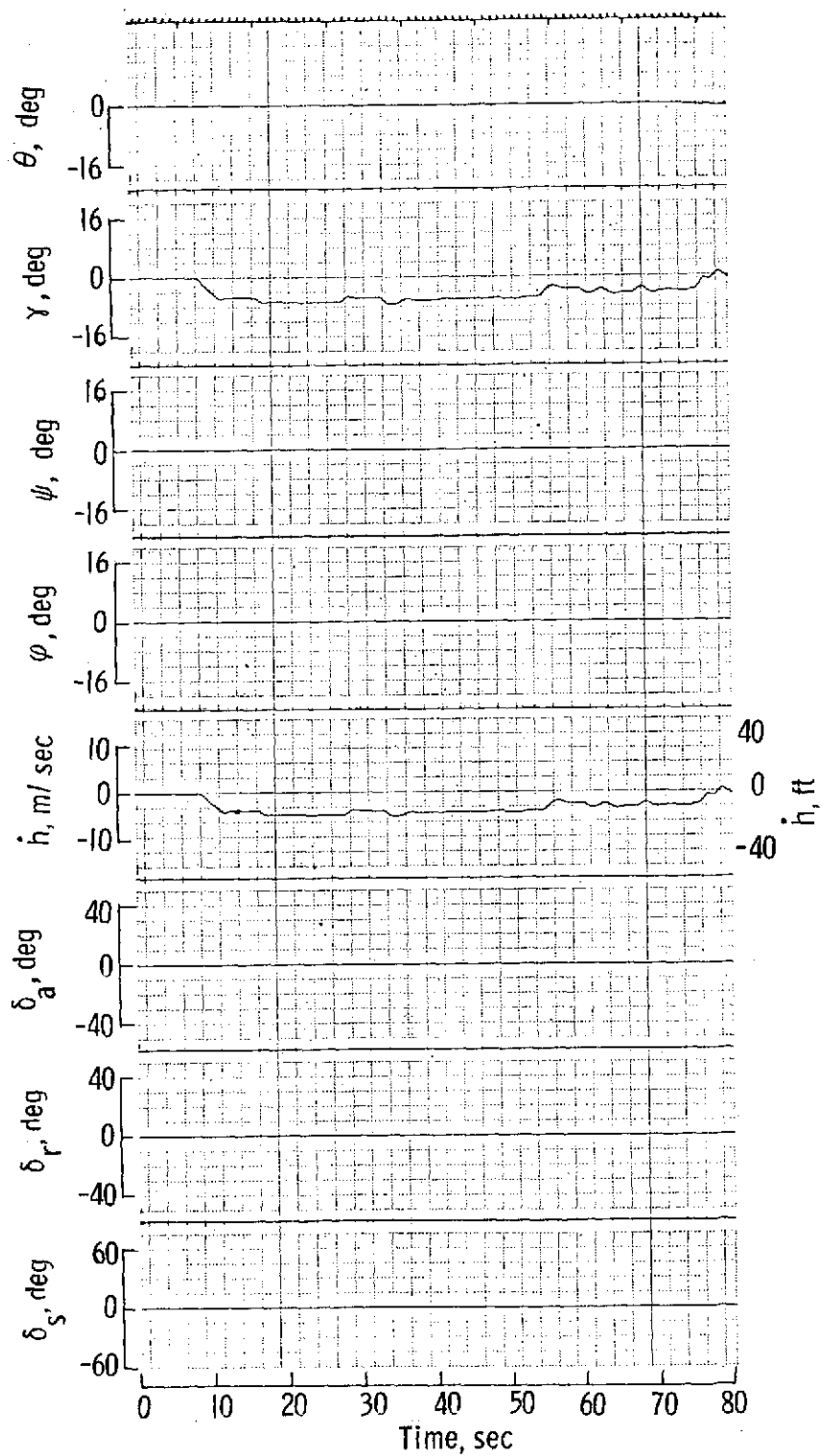


Figure 15. - Continued.

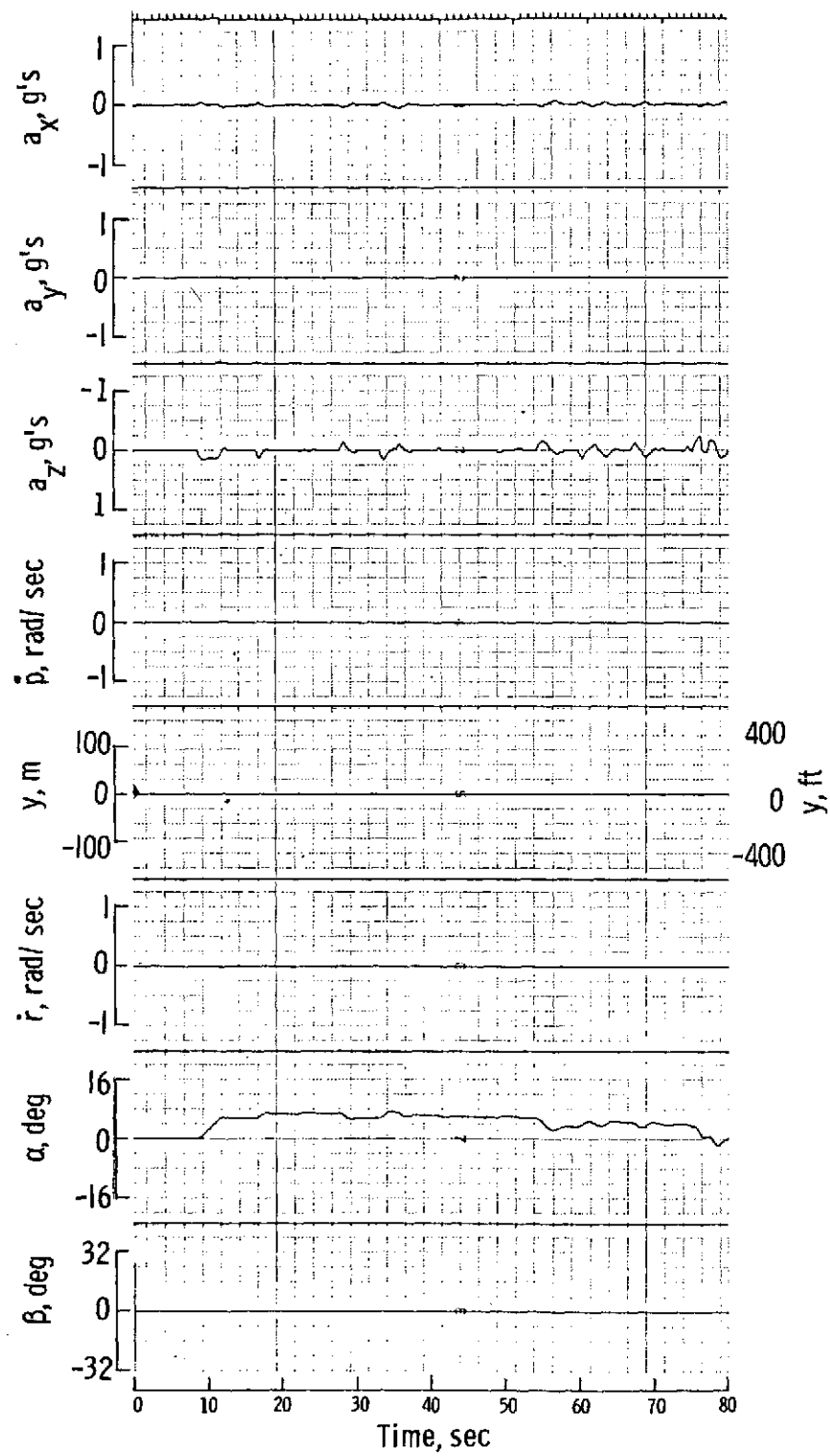


Figure 15.- Concluded.

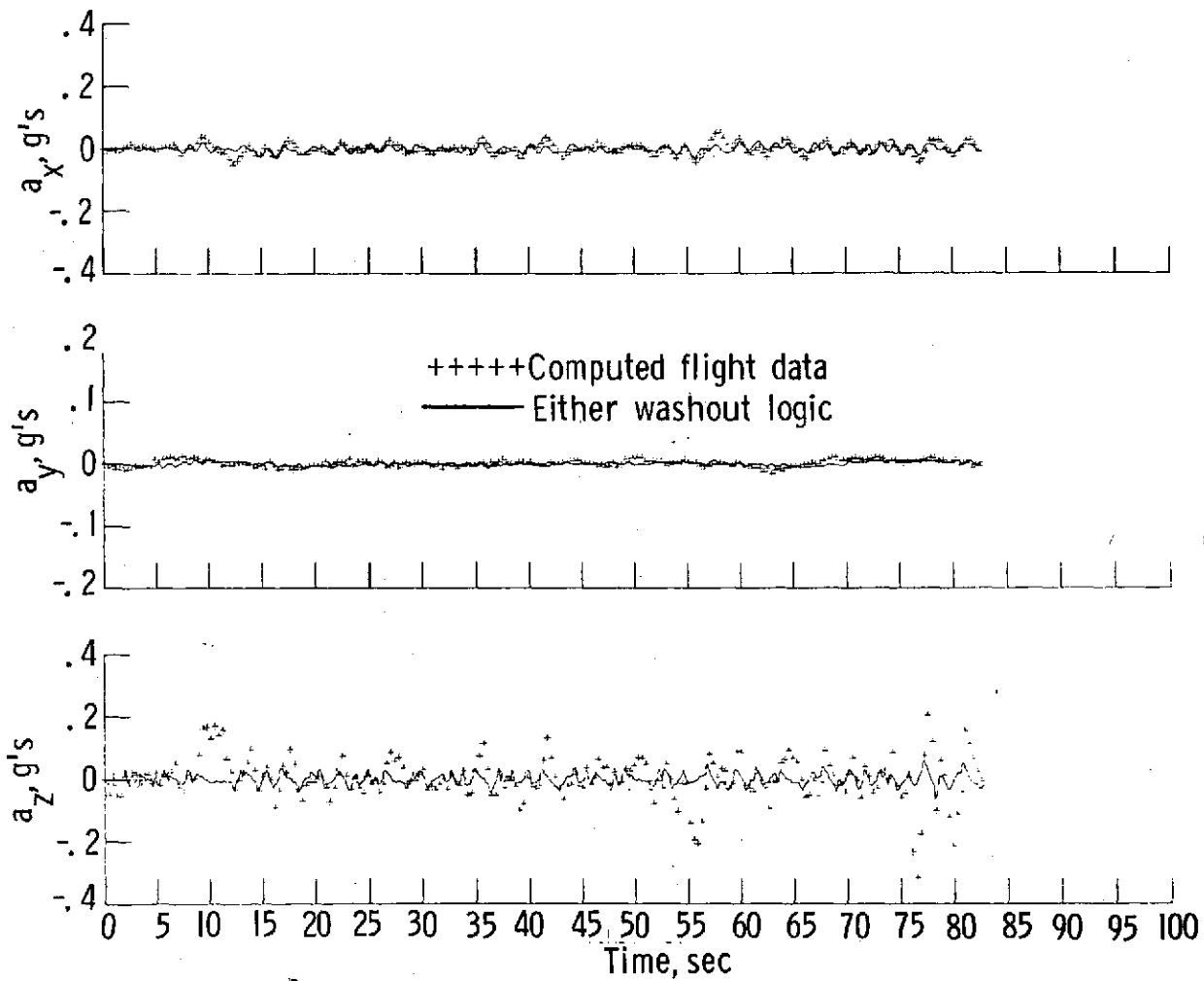


Figure 16.- Computed motion-base output for typical landing approach made in low-level turbulence (using either constraint logic).

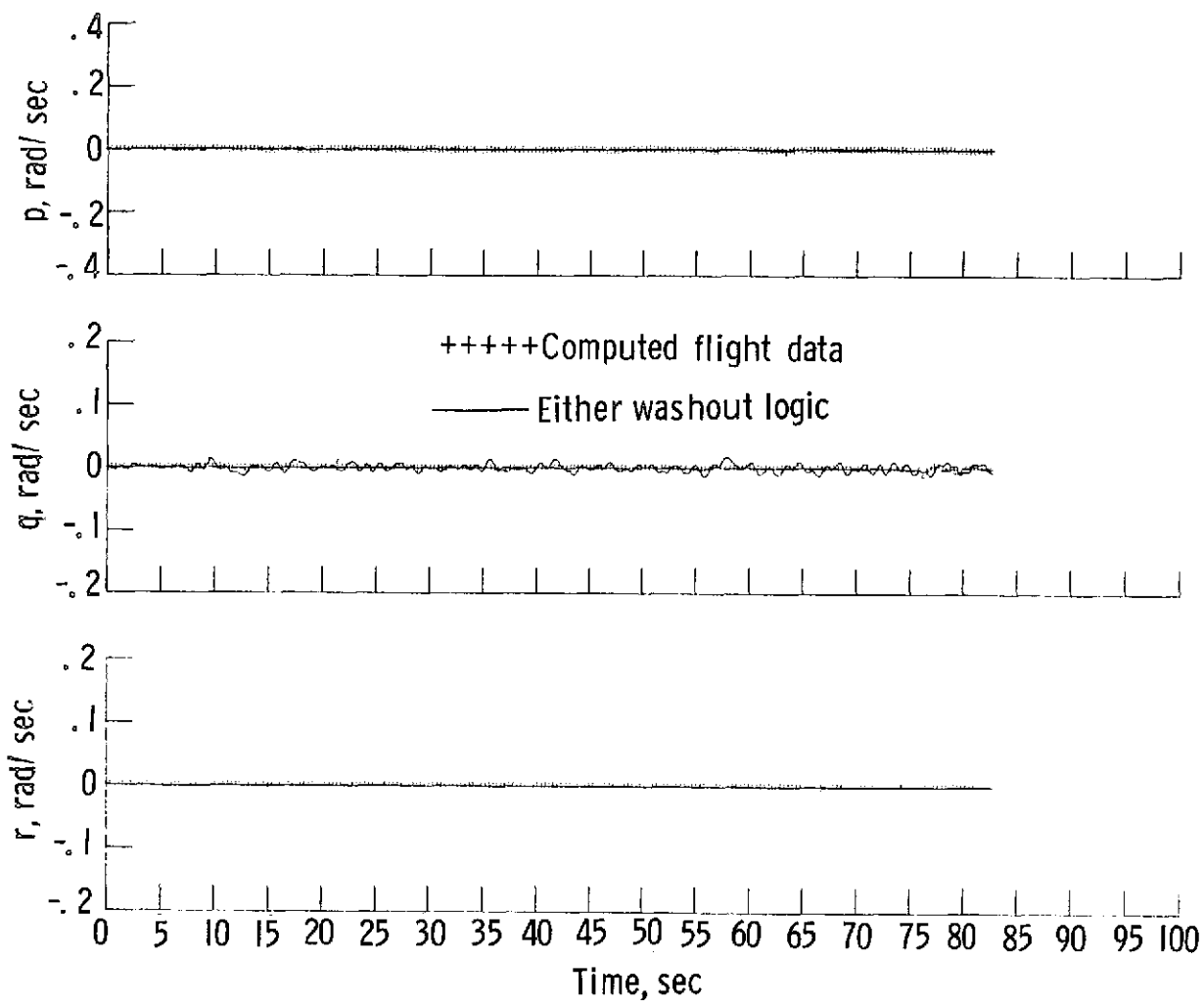


Figure 16.- Continued.

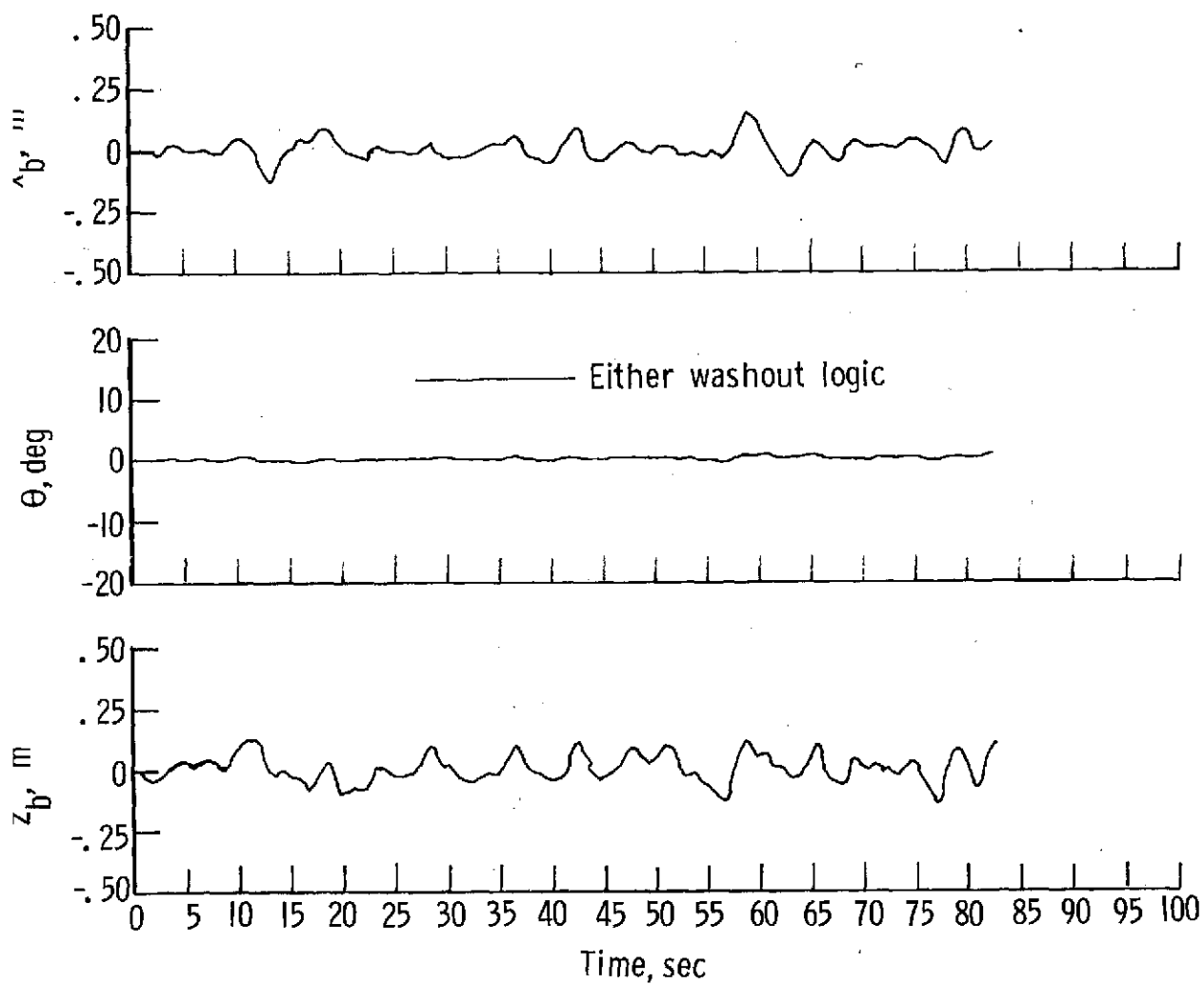


Figure 16.- Continued.

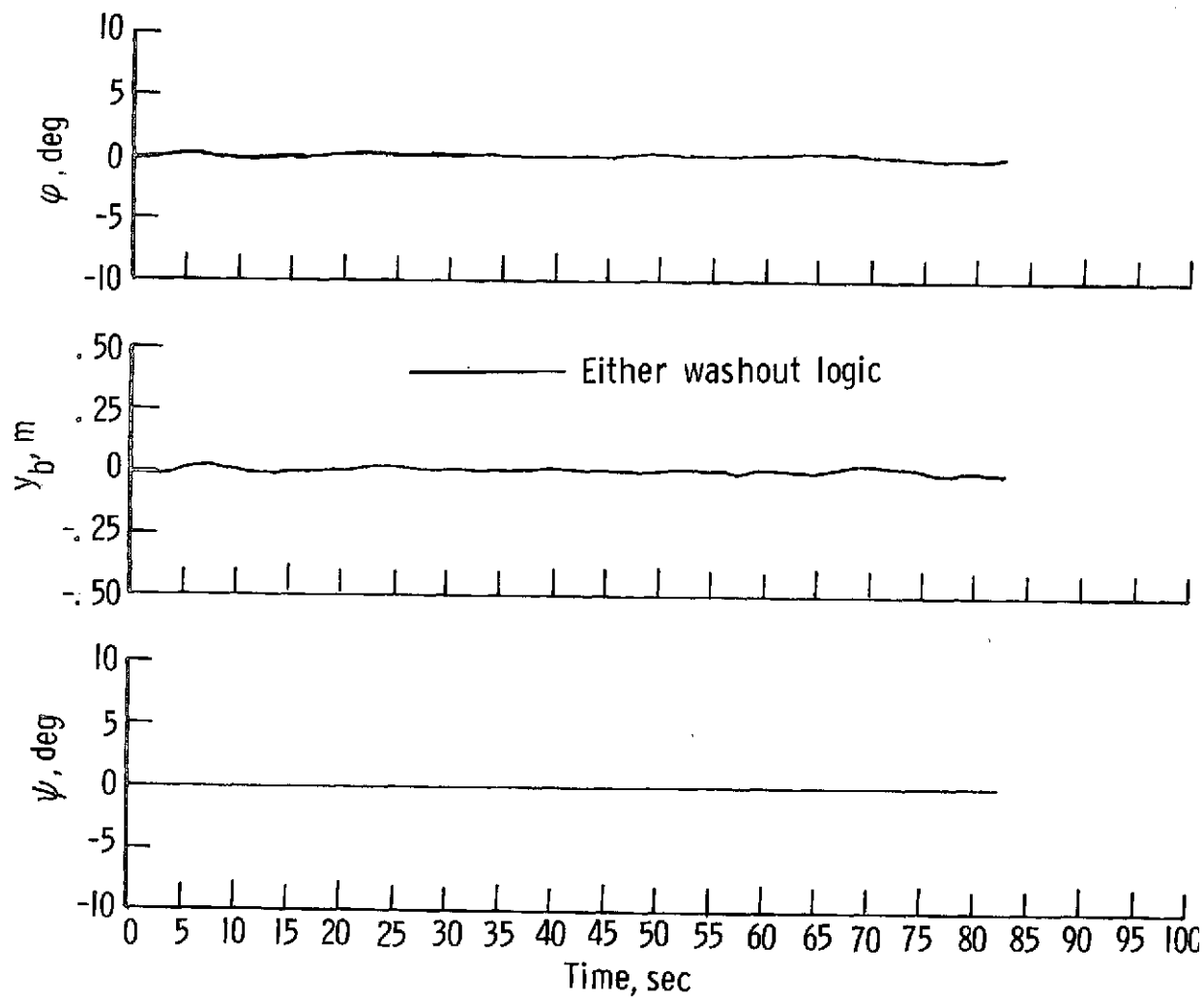


Figure 16.- Concluded.



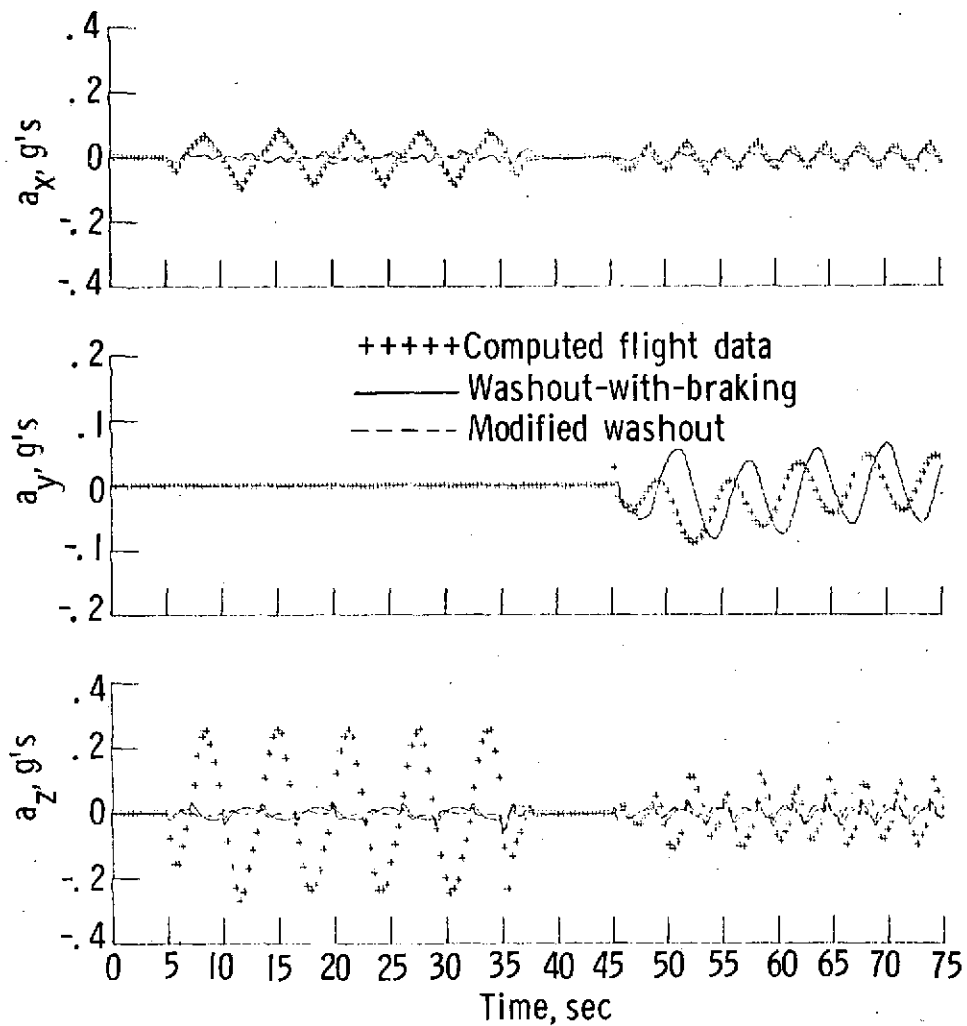


Figure 17.- Computed motion-base output for sinusoidal commands in flight-path angle and yaw rate.

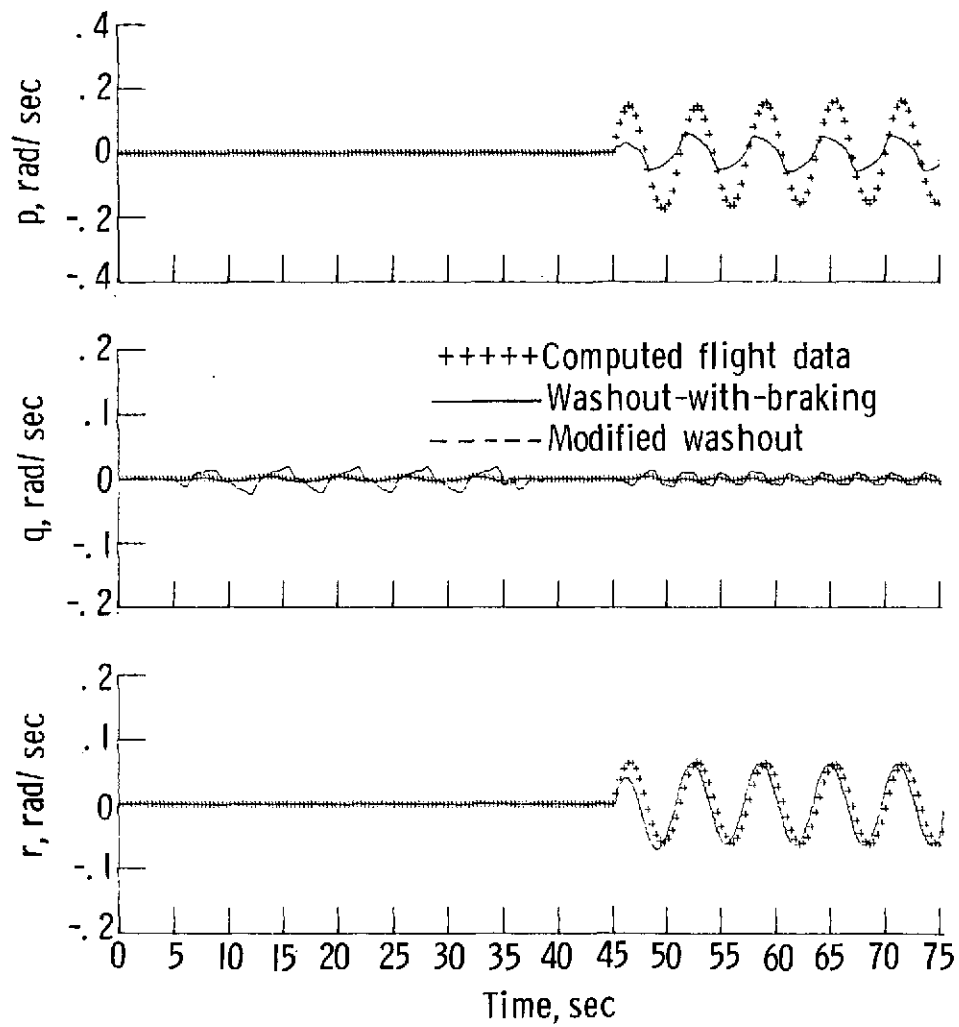


Figure 17.- Concluded.

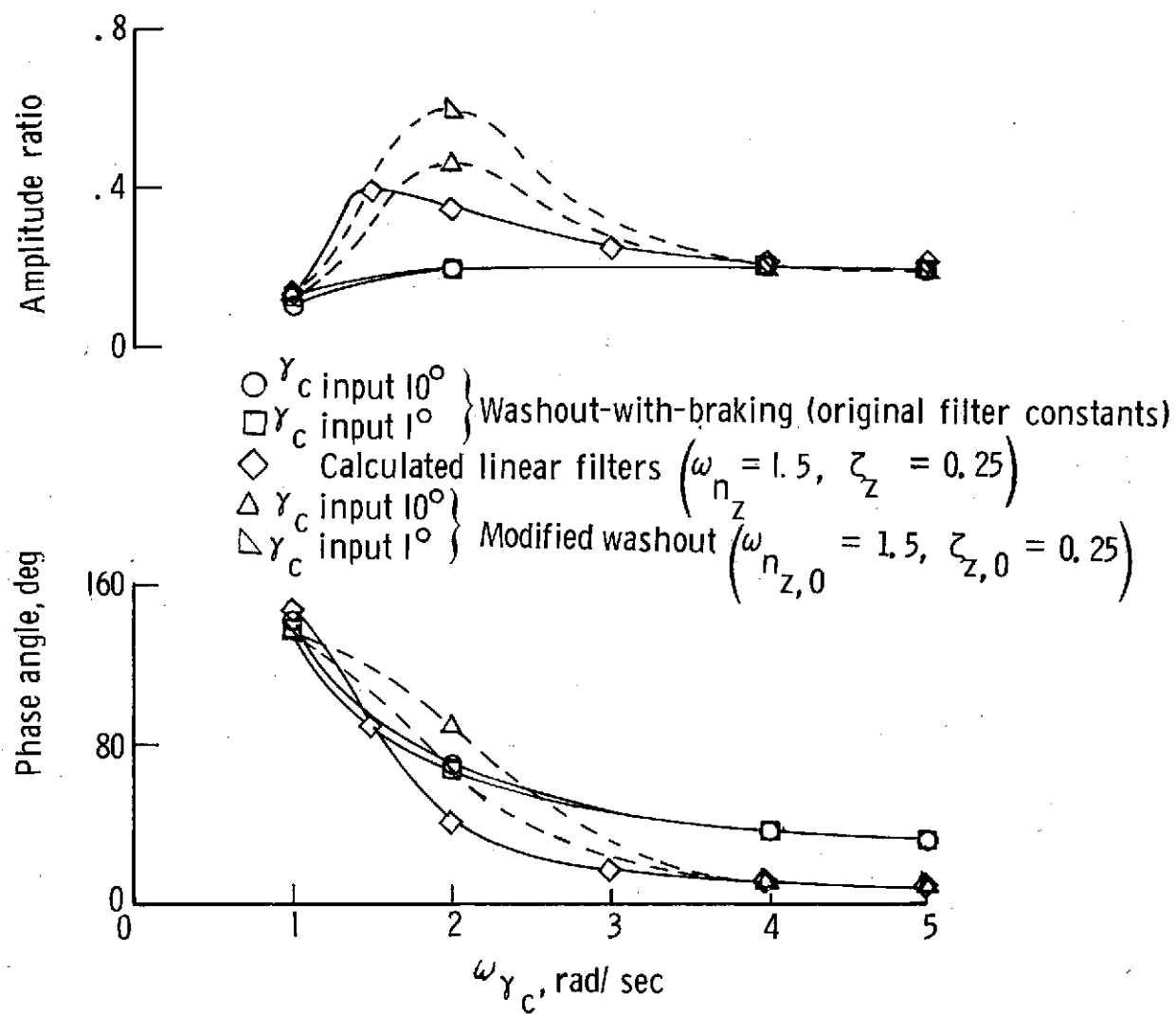


Figure 18.- Frequency-response comparison of washout-with-braking and modified washout (with reduced filter parameters) for the vertical channel.

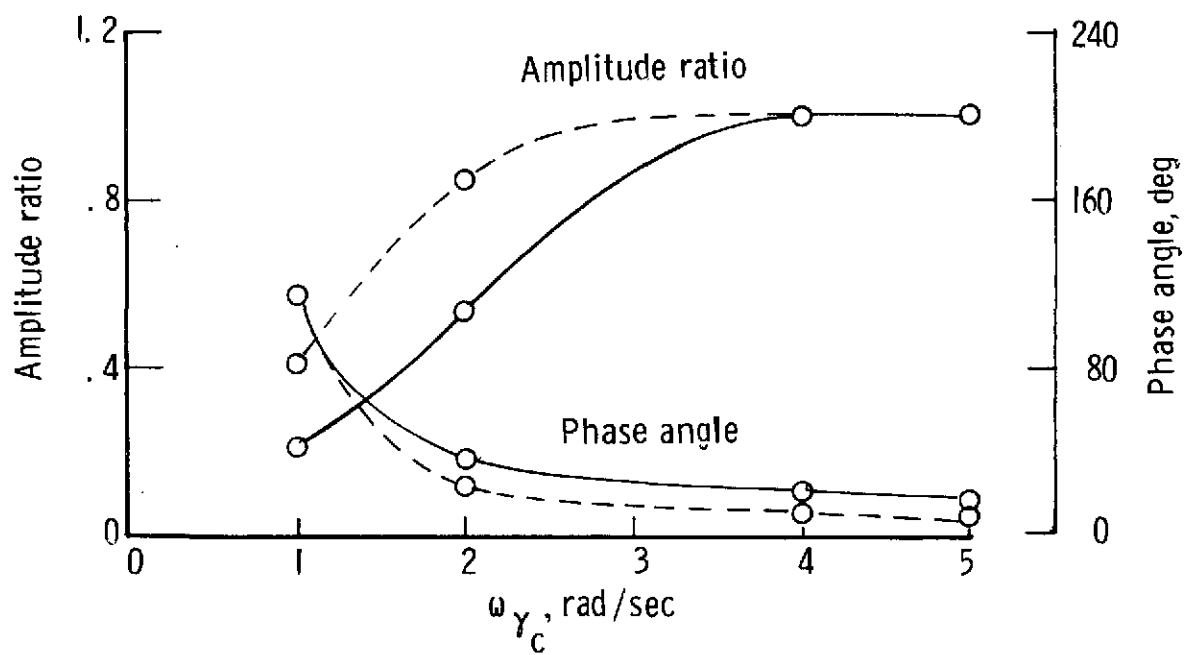


Figure 19.- Frequency response in the longitudinal channel for a  $3^\circ$  amplitude sinusoidal input in  $\gamma_c$ . Solid line denotes washout-with-braking (original filter parameters) and dashed line denotes modified washout ( $\omega_{n_{x,0}} = 1.0$ ,  $\zeta_{x,0} = 0.35$ ).

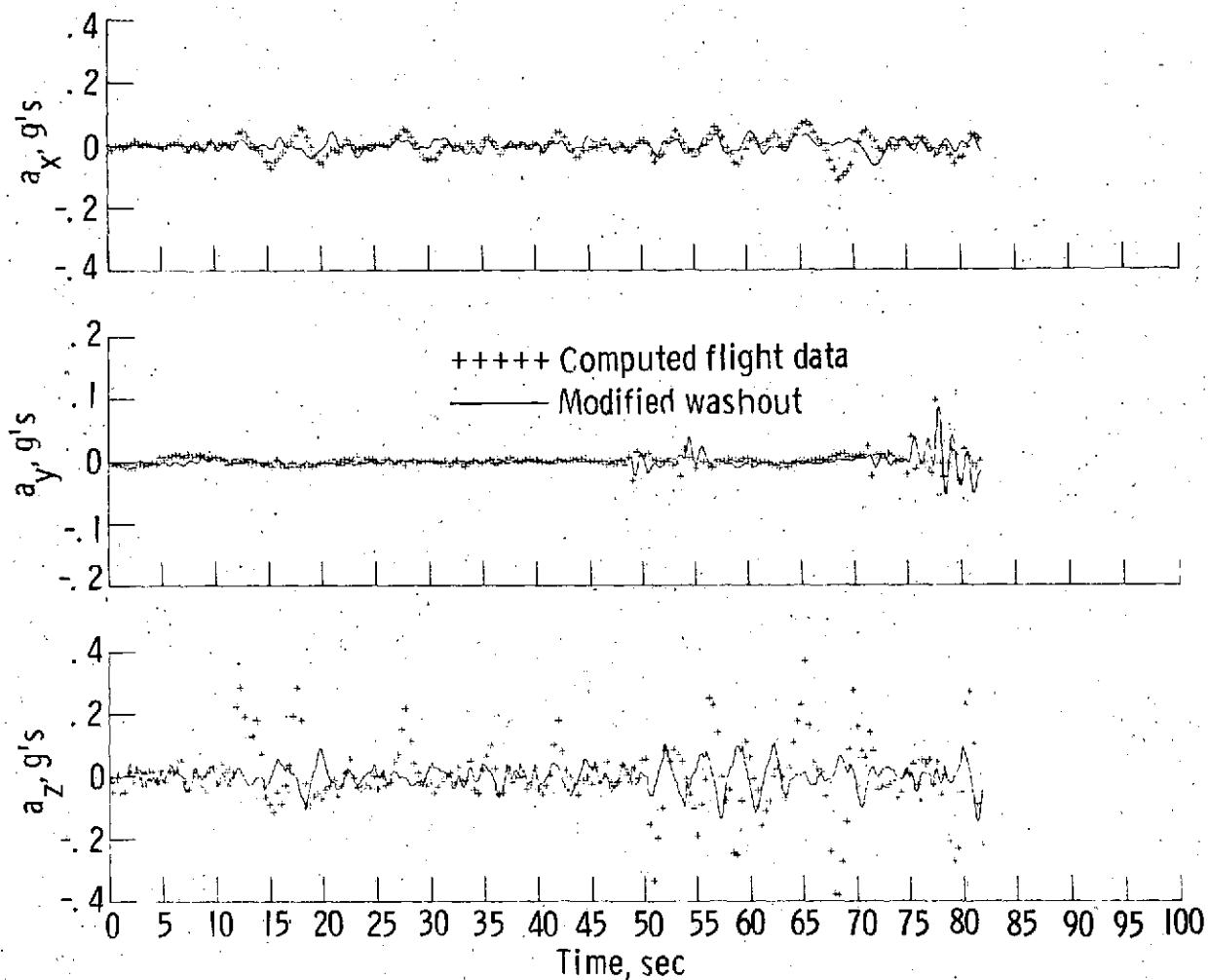


Figure 20.- Computed motion-base output for a typical flight in low-level turbulence.  
 (Modified washout logic has the basic values of  $\omega_{n_x}$  and  $\omega_{n_y}$  multiplied by 0.707,  $\omega_{n_z}$  by 0.5, and all the  $\xi$ 's by 0.5.)

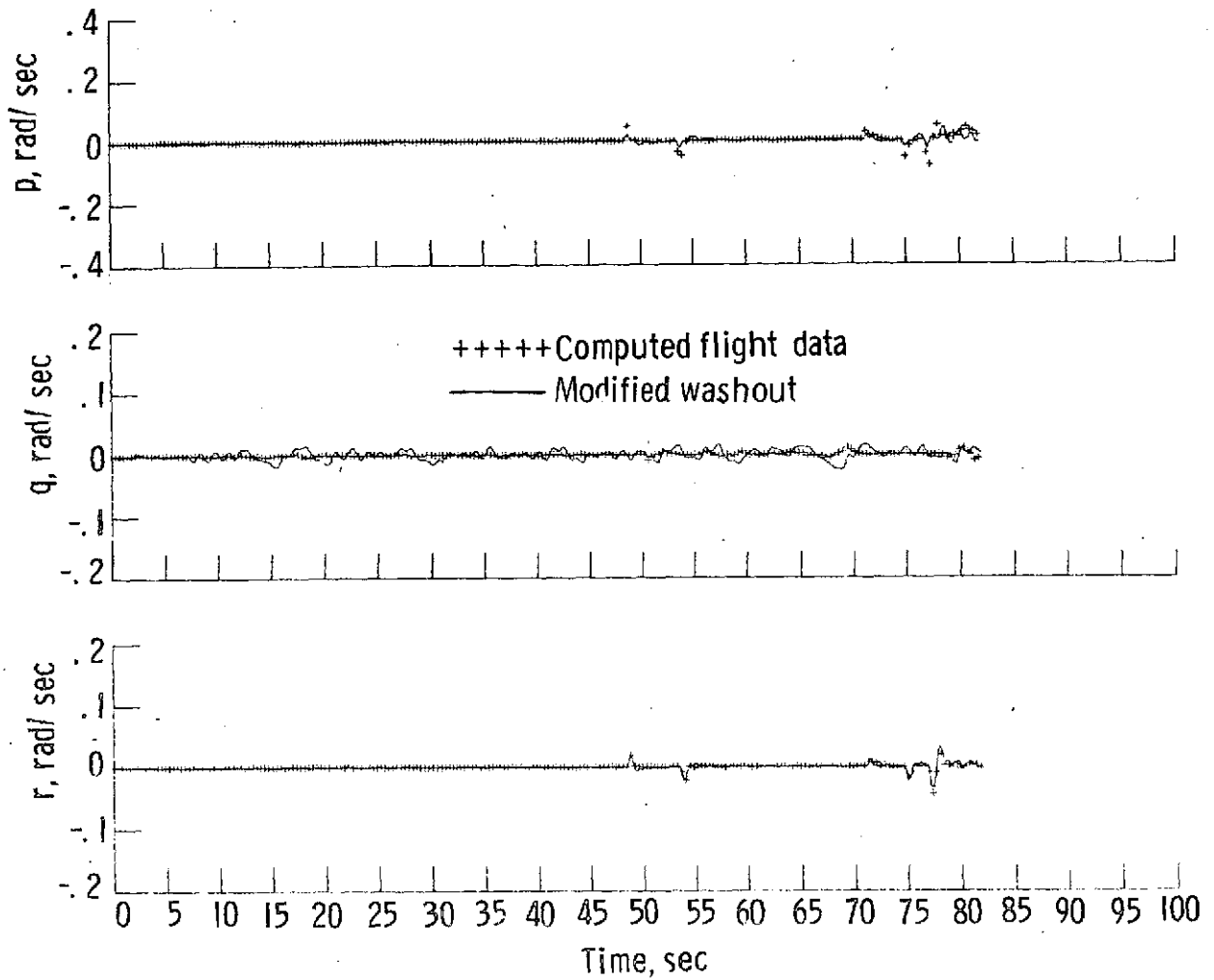


Figure 20. - Continued.

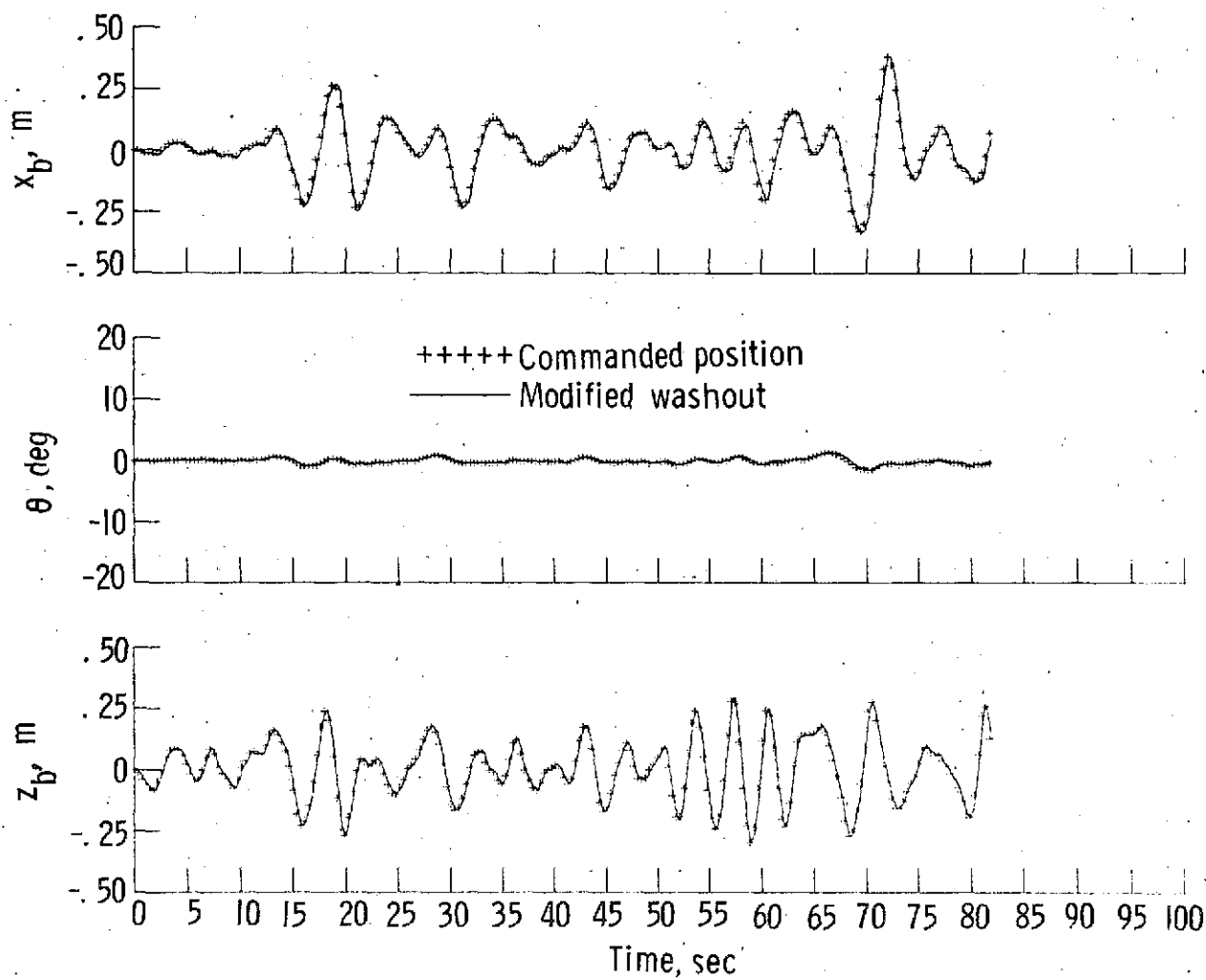


Figure 20.- Concluded.